



ATTACHMENT 5

**Holtec International Report No. HI-2125245, Revision 2
"Licensing Report for Quad Cities Criticality Analysis for Inserts –
Non Proprietary Version"**



Holtec Center, 555 Lincoln Drive West, Marlton, NJ 08053

Telephone (856) 797- 0900

Fax (856) 797 - 0909

***Licensing Report for Quad Cities Criticality
Analysis for Inserts - Non Proprietary Version***

FOR

Exelon

Holtec Report No: HI-2125245

Holtec Project No: 2127

Sponsoring Holtec Division: HTS

Report Class : SAFETY RELATED

HOLTEC INTERNATIONAL

Summary of Revisions:

Revision 0: Original Issue

Revision 1: Supplement 1 was added to cover a new revision of NETCO-SNAP-IN[®] rack insert.

Revision 2: All Revision 1 revision bars were removed. No other changes were made.

Table of Contents

1. INTRODUCTION	10
2. METHODOLOGY	11
2.1 GENERAL APPROACH	11
2.2 COMPUTER CODES AND CROSS SECTION LIBRARIES	11
2.2.1 MCNP5-1.51	11
2.2.1.1 MCNP5-1.51 Validation	11
2.2.1.1.1 [REDACTED]	12
2.2.2 CASMO-4	13
2.3 ANALYSIS METHODS	13
2.3.1 <i>Design Basis Fuel Assembly</i>	13
2.3.1.1 Peak Reactivity	14
2.3.1.1.1 Peak Reactivity and Fuel Assembly Burnup.....	14
2.3.1.1.2 [REDACTED]	14
2.3.1.2 [REDACTED]	15
2.3.1.3 Determination of the Design Basis Fuel Assembly Lattice.....	16
2.3.1.4 Optima2 CASMO-4 Model Simplification Effect.....	16
2.3.1.5 Core Operating Parameters	18
2.3.1.5.1 Reactor Power Uprate.....	18
2.3.1.5.2 Integral Reactivity Control Devices.....	19
2.3.1.5.3 Axial and Planar Enrichment Variations	19
2.3.1.5.4 Fuel Assembly De-Channeling.....	19
2.3.1.6 [REDACTED]	20
2.3.2 <i>Reactivity Effect of Spent Fuel Pool Water Temperature</i>	20
2.3.3 <i>Fuel Depletion Calculation Uncertainty</i>	21
2.3.4 <i>Fuel and Storage Rack Manufacturing Tolerances</i>	22
2.3.4.1 Fuel Manufacturing Tolerances	22
2.3.4.2 SFP Storage Rack Manufacturing Tolerances.....	23
2.3.5 <i>Radial Positioning</i>	23
2.3.5.1 Fuel Assembly Orientation in the Core.....	23
2.3.5.2 Fuel Radial Positioning in the Rack.....	23
2.3.5.3 Inserts Radial Positioning	25
2.3.5.4 Fuel Orientation in SFP Rack Cell.....	25
2.3.6 [REDACTED]	25
2.3.6.1 [REDACTED]	26
2.3.6.1.1 [REDACTED]	26
2.3.6.1.2 [REDACTED]	27
2.3.6.2 [REDACTED]	27
2.3.7 <i>Insert Coupon Measurement Uncertainty</i>	27
2.3.8 <i>Maximum k_{eff} Calculation for Normal Conditions</i>	27
2.4 MARGIN EVALUATION.....	28
2.5 FUEL MOVEMENT, INSPECTION AND RECONSTITUTION OPERATIONS	29
2.6 ACCIDENT CONDITION.....	29
2.6.1 <i>Temperature and Water Density Effects</i>	30
2.6.2 <i>Dropped Assembly – Horizontal</i>	30
2.6.3 <i>Dropped Assembly – Vertical into a Storage Cell</i>	30
2.6.4 <i>Storage Cell Distortion</i>	31
2.6.5 <i>Misloaded Fuel Assembly/Missing Insert</i>	31
2.6.6 <i>Mislocated Fuel Assembly</i>	32
2.6.6.1 Mislocation of a Fuel Assembly in the Water Gap between the Racks and Pool Wall	32
2.6.6.2 Mislocation of a Fuel Assembly in the Corner between Two Racks.....	32
2.6.6.3 Mislocation of a Fuel Assembly between the SFP Rack and the Inspection Platform	32
2.6.7 <i>Mis-installment of an Insert on Wrong Side of a Cell</i>	33

2.6.8	<i>Insert Mechanical Wear</i>	33
2.6.9	<i>Rack Movement</i>	33
2.7	[REDACTED]	33
2.7.1	[REDACTED]	35
2.8	SPENT FUEL RACK INTERFACES	36
2.9	RECONSTITUTED FUEL ASSEMBLIES	36
3.	ACCEPTANCE CRITERIA	37
3.1	APPLICABLE CODES, STANDARDS AND GUIDANCE'S	37
4.	ASSUMPTIONS	38
5.	INPUT DATA	39
5.1	FUEL ASSEMBLY SPECIFICATION	39
5.2	REACTOR PARAMETERS	39
5.3	SPENT FUEL POOL PARAMETERS	39
5.4	STORAGE RACK SPECIFICATION	40
5.4.1	<i>Material Compositions</i>	40
6.	COMPUTER CODES	41
7.	ANALYSIS	42
7.1	DESIGN BASIS AND UNCERTAINTY EVALUATIONS	42
7.1.1	[REDACTED]	42
7.1.2	<i>Determination of the Design Basis Fuel Assembly Lattice</i>	42
7.1.2.1	Fuel Assembly De-Channeling	42
7.1.3	<i>Optima2 CASMO-4 Model Simplification Effect</i>	42
7.1.4	<i>Core Operating Parameters</i>	43
7.1.4.1	Reactor Power Uprate	43
7.1.5	<i>Water Temperature and Density Effect</i>	43
7.1.6	<i>Depletion Uncertainty</i>	43
7.1.7	<i>Fuel and Rack Manufacturing Tolerances</i>	44
7.1.7.1	Fuel Assembly Tolerances	44
7.1.7.2	SFP Rack Tolerances	44
7.1.8	<i>Radial Positioning</i>	44
7.1.8.1	Fuel Assembly Radial Positioning in SFP Rack	44
7.1.8.2	Fuel Orientation in SFP Rack	44
7.1.9	<i>Fuel Rod Geometry Change</i>	45
7.1.9.1	[REDACTED]	45
7.1.9.2	[REDACTED]	45
7.1.10	[REDACTED]	45
7.2	MAXIMUM K_{EFF} CALCULATIONS FOR NORMAL CONDITIONS	45
7.3	MARGIN EVALUATION	45
7.4	ABNORMAL AND ACCIDENT CONDITIONS	46
7.5	MAXIMUM K_{EFF} CALCULATIONS FOR ABNORMAL AND ACCIDENT CONDITIONS	46
7.6	[REDACTED]	46
7.7	SPENT FUEL RACK INTERFACES	47
8.	CONCLUSION	48
9.	REFERENCES	49



Supplement 1: Additional Calculations to Support the Revised NETCO-SNAP-IN® Rack Insert
DesignS1-1

List of Tables

Table	Description	Page
Table 2.1(a)	Summary of the Area of Applicability of the MCNP5-1.51 Benchmark	51
Table 2.1(b)	Analysis of the MCNP5-1.51 calculations	52
Table 2.1(c)	[REDACTED]	53
Table 5.1(a)	[REDACTED]	54
Table 5.1(b)	[REDACTED]	55
Table 5.1(c)	[REDACTED]	56
Table 5.1(d)	[REDACTED]	57
Table 5.1(e)	[REDACTED]	58
Table 5.2(a)	Reactor Core and Spent Fuel Pool Parameters	59
Table 5.2(b)	Reactor Control Blade Data	60
Table 5.2(c)	[REDACTED]	61
Table 5.3(a)	Fuel Rack Parameters and Dimensions	62
Table 5.3(b)	Fuel Rack Insert Parameters and Dimensions	63
Table 5.4(a)	Non-Fuel Material Compositions	64
Table 5.4(b)	Summary of the Fuel and Fission Product Isotopes Used in Calculations	65
Table 7.1(a)	[REDACTED]	66
Table 7.1(b)	[REDACTED]	67
Table 7.1(c)	[REDACTED]	68
Table 7.2(a)	Results of the MCNP5-1.51 Calculations for SVEA-96 Optima2 QI22 Lattices	69
Table 7.2(b)	Results of the MCNP5-1.51 Calculations for GE14 Lattice Type 5	71
Table 7.3	Results of the MCNP5-1.51 Calculations for Design Basis and Simplified Model of SVEA-96 Optima2 QI22 Lattice Type 146	72
Table 7.4	Results of the MCNP5-1.51 Calculations for Core Operating Parameters	73
Table 7.5	Results of the MCNP5-1.51 Calculations for the Effect of Water Temperature and Density	74
Table 7.6(a)	Results of the MCNP5-1.51 Calculations for the Depletion Uncertainty	75
Table 7.6(b)	[REDACTED]	76
Table 7.7	Results of the MCNP5-1.51 Calculations for Fuel Tolerances	77
Table 7.8	Results of the MCNP5-1.51 Calculations for Rack Tolerances	78

Table	Description	Page
[REDACTED]	[REDACTED]	[REDACTED]
Table S1-1	Fuel Rack Insert Revised Dimensions	S1-5
Table S1-2	Results of the MCNP5 Calculations for Revised Rack Tolerances	S1-6
Table S1-3	Results of the MCNP5-1.51 Calculations for Revised Fuel Radial Positioning in SFP Racks	S1-7
Table S1-4	Results of the MCNP5-1.51 Calculations for Revised Fuel Orientation in SFP Racks	S1-8
Table S1-5	Maximum keff Calculation for Normal Conditions in Revised SFP Racks	S1-9
Table S1-6	Maximum keff Calculation for the Bounding Accident Condition in Revised SFP Racks	S1-10

List of Figures

Figure	Description	Page
Figure 2.1	2-D representation of the CASMO-4 models of SVEA-96 Optima2 QI22 lattices (a) Lattice type 146; (b) lattice type 147; (c) lattice type 148; (d) lattice type 149; (e) lattice type 150; (f) lattice type 151.	93
Figure 2.2	2-D representation of the CASMO-4 models of GE14 lattices (a) Lattice type 2; (b) lattice type 3; (c) lattice type 4; (d) lattice type 5.	94
Figure 2.3	2-D representation of the CASMO-4 models of GE 8x8 lattices (a) Lattice 854; (b) lattice 855.	95
Figure 2.4	2-D representation of the CASMO-4 models of GE 7x7 lattices (a) Lattice type V; (b) lattice type W.	96
Figure 2.5	2-D representation of the CASMO-4 models of ATRIUM 9B lattices (a) Lattice SPCA9-3.96L-10G6.5; (b) lattice SPCA9-3.96L-11G6.5; (c) lattice SPCA9-3.96L-11G5.5.	97
Figure 2.6(a)	2-D representation of CASMO-4 SVEA-96 Optima2 QI22 model used for depletion analyses.	98
Figure 2.6(b)	2-D representation of MCNP5-1.51 SVEA-96 Optima2 QI22 model equivalent of the CASMO-4 model.	99
Figure 2.6(c)	2-D representation of MCNP5-1.51 SVEA-96 Optima2 QI22 model used in criticality calculations.	100
Figure 2.7	2-D representation of the MCNP5-1.51 SFP racks radial positioning for the 2x2 array models (a) Cell centered positioning; (b) every fuel assembly is positioned toward the center; (c) every fuel assembly is positioned toward the corner where the insert wings connect; (d) every fuel assembly is positioned away from the corner where the insert wings connect; (e) every fuel assembly is middle between insert and cell walls.	101
Figure 2.8	2-D representation of the MCNP5-1.51 SFP racks radial positioning for the 8x8 array model Every fuel assembly is positioned toward the center.	102
Figure 2.9	2-D representation of the MCNP5-1.51 fuel orientation in SFP rack cell for the 2x2 array models (a) The reference case; (b) through (e) the other evaluated cases.	103
Figure 2.10(a)	A 2-D representation of the MCNP5-1.51 model of misloaded fuel assembly/missing insert (eccentric).	104
Figure 2.10(b)	A 2-D representation of the MCNP5-1.51 model of misloaded fuel assembly/missing insert (cell centered).	105

Figure	Description	Page
Figure 2.11(a)	A 2-D representation of the MCNP5-1.51 model of mislocated fuel assembly in the corner between two racks.	106
Figure 2.11(b)	A 2-D representation of the MCNP5-1.51 model of mislocated fuel assembly in the corner between two racks (eccentric).	107
Figure 2.11(c)	A 2-D representation of the MCNP5-1.51 model of mislocated fuel assembly in the corner between two racks (cell centered).	108
Figure 2.12(a)	A 2-D representation of the MCNP5-1.51 model of mislocated fuel assembly adjacent to the platform (eccentric).	109
Figure 2.12(b)	A 2-D representation of the MCNP5-1.51 model of mislocated fuel assembly adjacent to the platform (cell centered).	110
Figure 2.13	2-D representation of the MCNP5-1.51 SFP racks radial positioning of the GE14 fuel assemblies for the 2x2 array models (a) Cell centered positioning with fuel channel; (b) Cell centered positioning. without fuel channel; (c) every fuel assembly without fuel channel is moved toward the center; (d) every fuel assembly without fuel channel is moved away from the corner where the insert wings connect.	111
Figure 5.1	A 2-D representation of the CASMO-4 model of the SVEA-96 Optima2 fuel lattice 146 in the core.	112
Figure 5.2(a)	Quad Cities Unit 1 SFP.	113
Figure 5.2(b)	Quad Cities Unit 2 SFP.	114
Figure 5.3	Insert cross section profile.	115
Figure 5.4	A 2-D representation of the MCNP5-1.51 model of the SFP rack cell with insert.	116
Figure 7.1	[REDACTED]	117
Figure 7.2	[REDACTED]	118
Figure 7.3	[REDACTED]	119
[REDACTED]	[REDACTED]	[REDACTED]

Figure	Description	Page
Figure S1-1	Insert cross section profile	S1-11

1. INTRODUCTION

This report documents the criticality safety evaluation for the storage of spent BWR fuel in the Unit 1 and Unit 2 spent fuel pools (SFPs) at Quad Cities Station operated by Exelon. The Unit 1 and Unit 2 SFP racks are identical and are designed to accommodate BWR fuel. Currently, the SFP racks credit BORAFLEX for reactivity control. This new analysis will not credit the BORAFLEX but will instead credit new NETCO-SNAP-IN[®] rack inserts, which are new to Quad Cities but not new relative to their use for spent fuel pool reactivity control. This analysis will demonstrate that with credit for the inserts the effective neutron multiplication factor (k_{eff}) in the SFP racks fully loaded with fuel of the highest anticipated reactivity, at a temperature corresponding to the highest reactivity, is less than 0.95 with a 95% probability at a 95% confidence level. Reactivity effects of abnormal and accident conditions are also evaluated to assure that under all credible abnormal and accident conditions, the reactivity will not exceed the regulatory limit.

Criticality control in the SFP, as credited in this analysis, relies on the following:

- Fixed neutron absorbers
 - NETCO-SNAP-IN[®] rack inserts in SFP rack cells
- Integrated neutron absorbers
 - Gadolinium (Gd) in the fuel (peak reactivity isotopic composition).

Criticality control in the SFP, as credited in this analysis, does not rely on the following:

- Burnup credit
- BORAFLEX.

2. METHODOLOGY

2.1 General Approach

The analysis is performed consistent with regulatory requirements and guidance. The calculations are performed using either the worst case bounding approach or the statistical analysis approach with respect to the various calculation parameters. The approach considered for each parameter is discussed below.

2.2 Computer Codes and Cross Section Libraries

2.2.1 MCNP5-1.51

MCNP5-1.51 is a three-dimensional Monte Carlo code developed at the Los Alamos National Laboratory [1]. MCNP5-1.51 calculations use continuous energy cross-section data based on ENDF/B-VII. MCNP is selected because it has history of successful use in fuel storage criticality analyses and has most of the necessary features (except for fuel depletion analysis) for the analysis to be performed for Quad Cities Station SFP.

The convergence of a Monte Carlo criticality problem is sensitive to the following parameters: (1) number of histories per cycle, (2) the number of cycles skipped before averaging, (3) the total number of cycles and (4) the initial source distribution. All MCNP5 calculations are performed with a minimum of 12,000 histories per cycle, a minimum of 150 skipped cycles before averaging, and a minimum of 150 cycles that are accumulated. The initial source is specified as uniform over the fueled regions (assemblies). [REDACTED]

2.2.1.1 MCNP5-1.51 Validation

[REDACTED]

[REDACTED]

[REDACTED]

[Redacted]

[Redacted]

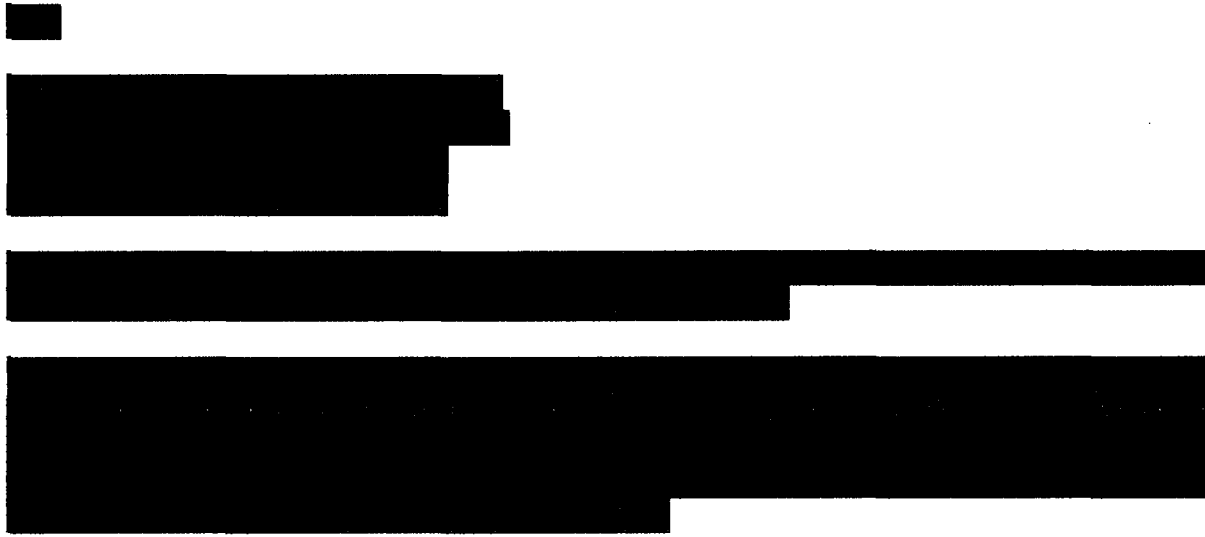
[Redacted]

2.2.1.1.1 [Redacted]

[Redacted]

[Redacted]

[Redacted]



2.2.2 CASMO-4

Fuel depletion analyses during core operation are performed with CASMO-4 Version 2.05.14 (using the 70-group cross-section library), which has been approved by the NRC for reactor analysis (depletion) when providing reactivity data for specific 3D simulator codes. CASMO-4 is a two-dimensional multigroup transport theory code based on the Method of Characteristics and it is developed by Studsvik of Sweden [4]. CASMO-4 is used to perform depletion calculations and to perform various sensitivity studies. The uncertainty on the isotopic composition of the fuel (i.e., the number density) is considered as discussed below (see Section 2.3.3). A validation for CASMO-4 to develop a bias and bias uncertainty is not necessary because the results of the CASMO-4 sensitivity studies are not used as input into the k_{eff} calculations. However, the code authors have validated CASMO-4 against MCNP and various critical experiments [5].

The version of the CASMO-4 code used in this application has a built-in limitation in a number of isotopes that may be extracted for specific pins. Therefore, two independent CASMO-4 depletion calculations were performed to separately extract the actinides and fission products. The extracted isotopes were further combined and used in MCNP5-1.51 calculations.

2.3 Analysis Methods

2.3.1 Design Basis Fuel Assembly

There are various fuel designs stored in the Quad Cities SFP. For the purpose of this analysis, the reactivity of each design is evaluated and the most reactive fuel bundle lattice is determined for use as the design basis fuel assembly to determine k_{eff} at the 95/95 level. This approach follows the guidance in [2] and [6], and is further described below.

2.3.1.1 Peak Reactivity

The BWR fuel designs used at the Quad Cities Station use Gd as an integral burnable absorber. Initially, the Gd in the fuel assembly holds down the fresh fuel assembly reactivity and then, as core depletion occurs, the Gd begins to burnout until it is essentially fully depleted. As the Gd depletes the reactivity of the fuel assembly increases until it reaches a peak. This peak reactivity is the fuel assembly's most reactive condition. Note that most BWR fuel designs are composed of various axial lattices (including blankets) that can have different axial lengths, uranium loadings (also mixed oxide loading, for MOX fuel), fuel pin arrangements including partial or part-length rods, Gd pin locations and loading, etc. These various lattice components can all effect at what burnup the peak reactivity occurs and the magnitude of the peak reactivity. The axial lattices within a single fuel assembly can therefore all have different peak reactivity.

[REDACTED]

[REDACTED]

2.3.1.1.1 Peak Reactivity and Fuel Assembly Burnup

Typically, a spent fuel assembly is characterized by its assembly average burnup (over all lattices or nodes). In this analysis methodology the fuel assembly average burnup is of no concern and is not credited for reactivity control. Rather, the methodology credits the residual Gd and other depletion isotopic compositions at the fuel assembly peak reactivity (most reactive lattice peak reactivity). While the peak reactivity occurs at some specific *lattice burnup*, the peak reactivity lattice burnup varies from lattice to lattice within a fuel design. Therefore, independent calculations with MCNP5-1.51 using pin specific compositions (see Section 2.3.1.1.2) are performed for *every lattice* of the SVEA-96 Optima2 fuel assembly (as will be seen in Section 7, this is the fuel assembly with the design basis lattice) over a burnup range to determine the burnup at peak reactivity for every lattice. Since each lattice is considered at its peak reactivity (and therefore the lattice or nodal burnup at which that occurs), the fuel assembly average burnup or fuel assembly burnup profile is not applicable because the analysis already considers each lattice at its most reactive composition, independent of the fuel assembly average burnup.

2.3.1.1.2 [REDACTED]

[REDACTED]

[REDACTED]

[REDACTED]

2.3.1.2 [REDACTED]

[REDACTED]

[REDACTED]

[REDACTED]

[REDACTED]

[REDACTED]

[REDACTED]

[REDACTED]

2.3.1.3 Determination of the Design Basis Fuel Assembly Lattice

[REDACTED]

[REDACTED]

2.3.1.4 Optima2 CASMO-4 Model Simplification Effect

As previously discussed in Section 2.3.1.2, various fuel designs were provided. Of these fuel designs, the SVEA-96 Optima2 designs were specified to be bounding. The Optima2 model in CASMO-4 is described as the SVEA-96 model provided in the CASMO-4 manual [4]. This CASMO-4 internal model is slightly different from the actual fuel assembly geometry. Therefore, it is important to evaluate and if necessary quantify the reactivity effect of the CASMO-4 model simplifications inherent in the code. The CASMO-4 model geometry of the SVEA-96 Optima2 fuel differs from the SVEA-96 Optima2 fuel as follows:

- [REDACTED]
- [REDACTED]
- [REDACTED]

With respect to the fuel assembly geometry models, the amount of zirconium (and therefore the amount of water) in the CASMO-4 model of the SVEA-96 Optima2 fuel is reasonably similar to that of the actual SVEA-96 Optima2 fuel and therefore these built-in CASMO-4 simplifications are acceptable. However, to evaluate the CASMO-4 model geometry simplification effect on reactivity, an applicable set of code-to-code comparisons is performed. The following cases are evaluated.

[REDACTED]

[REDACTED]

[REDACTED]

[REDACTED]

For the purpose of showing that the two codes calculate an equivalent reactivity the following comparisons are made:

- Case 2.3.1.4.1 is compared to Case 2.3.1.4.2 at 0 GWD/MTU to show that the two codes calculate similar results with respect to the fuel assembly and storage rack geometry.
- Case 2.3.1.4.1 is compared to Case 2.3.1.4.2 at peak reactivity burnup to quantify the reactivity difference due to the effect of the spent fuel. The two codes use different cross section library versions and calculation sequences. The main calculation sequence difference between the two codes is that CASMO-4 uses a thermal expansion of spent fuel pellet which effects the fuel density [4]. The actual density is conservatively used in MCNP5-1.51. The results are expected to show that the MCNP5-1.51 code is conservative with respect to the CASMO-4 code. Any non-conservative result would be treated as a bias.
- Case 2.3.1.4.3 is compared to Case 2.3.1.4.2 to show the reactivity difference between the simplified MCNP5-1.51 model and the design basis model that is slightly modified to be similar to the CASMO-4 insert orientation. This case is expected to show that the design basis model with respect to the fuel pin pitch (and subsequent sub-bundle pitch) is conservative. This is expected to be conservative because the design basis model fuel compositions are taken from the average fuel pin pitch CASMO-4 calculations and used in the MCNP5-1.51 design basis actual fuel pin locations. Any non-conservative result would be treated as a bias.

Case 2.3.1.4.3 is compared to the result of the actual design basis results (similar to Case 2.3.1.4.3 but with the bounding insert orientation) to show that the design basis model is conservative.

2.3.1.5 Core Operating Parameters

As previously discussed, CASMO-4 is used to perform depletion calculations to determine the spent fuel isotopic composition. The operating parameters for spent fuel depletion calculations are discussed in this Section. The operating parameters which may have a significant impact on BWR spent fuel isotopic composition are void fraction, control blade history, moderator temperature, fuel temperature, and power density. Other parameters such as axial enrichment distribution and effect of burnable absorbers are discussed in Section 2.3.1.5.3 and Section 2.3.1.5.2, respectively. Sensitivity studies are performed to show the effect of each individual parameter, and to confirm that the selected values are in fact appropriate when combined at their worst case.

2.3.1.5.1 Reactor Power Uprate

To determine the effect of the power uprate on the reactivity of fuel assemblies in the SFP racks, the following evaluations are performed.

- [REDACTED]

- [REDACTED]

2.3.1.5.2 Integral Reactivity Control Devices

The only type of burnable absorber used for the fuel assemblies covered in this analysis is Gd. The use of Gd does not increase the reactivity of the assembly, compared to an assembly lattice where all rods contain fuel and no Gd. As discussed in Section 2.3.1.1, the Gd in the fuel assembly holds down the fresh fuel assembly reactivity and then, as core depletion occurs, the Gd begins to burnout until it is essentially fully depleted. As the Gd depletes the reactivity of the fuel assembly increases until it reaches a peak. This peak reactivity is the fuel assembly's most reactive condition, which is used for design basis condition. Note that integrated absorbers do not change the amount of water in the assembly, which is a large part of the effect of non-integral absorbers.

2.3.1.5.3 Axial and Planar Enrichment Variations

2.3.1.5.4 Fuel Assembly De-Channeling

The SVEA-96 Optima2 fuel assembly (the most reactive fuel assembly, as will be shown in Section 7) cannot be de-channeled for storage in the SFP because of its specific design. However, GE14 (the most second reactive fuel assembly, as will be shown in Section 7) may be de-channeled. Studies are performed to evaluate the effect of storage of GE14 without the Zr channel at various radial positioning in the storage cells. The following cases are evaluated.

- Case 2.3.1.5.4.1: This is the reference for Case 2.3.1.5.4.2 through Case 2.3.1.5.4.4. The MCNP5-1.51 model used herein is a 2x2 array with the cell centered fuel assembly that includes the Zr channel, as shown in Figure 2.13(a).
- Case 2.3.1.5.4.2: The MCNP5-1.51 is a 2x2 array of GE14 fuel assembly lattice 5 (the most reactive lattice of GE14, as will be shown in Section 7). The Zr channel is removed, as shown in Figure 2.13(b). The fuel assemblies are cell centered.
- Case 2.3.1.5.4.3: The MCNP5-1.51 is the same as that of Case 2.3.1.5.4.2, except the fuel assemblies are eccentric toward the center, as shown in Figure 2.13(c).
- Case 2.3.1.5.4.4: The MCNP5-1.51 is the same as that of Case 2.3.1.5.4.2, except the fuel assemblies are eccentric away from the corner where the insert wings connect, as shown in Figure 2.13(d).

2.3.1.6 [REDACTED]

2.3.2 Reactivity Effect of Spent Fuel Pool Water Temperature

The Quad Cities Station SFP has a normal pool water temperature operating range below 150 °F. For the nominal condition, the criticality analyses are to be performed at the most reactive temperature and density [2]. Also, there are temperature-dependent cross section effects in MCNP5-1.51 that need to be considered. In general, both density and cross section effects may not have the same reactivity effect for all storage rack scenarios, since configurations with strong neutron absorbers typically show a higher reactivity at lower water temperature, while configurations without such neutron absorbers typically show a higher reactivity at a higher water temperature. For the SFP racks which credit inserts, the most reactive SFP water temperature and density is expected to be at 39.2 °F and 1 g/cc, respectively.

The standard cross section temperature in MCNP5-1.51 is 293.6 K. Cross sections are also available at other temperatures; however, not usually at the desired temperature for SFP criticality analysis. MCNP5-1.51 has the ability to automatically adjust the cross sections to the specified temperature when using the TMP card. Furthermore, MCNP5-1.51 has the ability to make a molecular energy adjustment for select materials (such as water) by using the S(α,β) card. The S(α,β) card is provided for certain fixed temperatures which are not always applicable to SFP criticality analysis. Rather, there are limited temperature options, i.e., 293.6 K and 350 K, etc. Additionally, MCNP5-1.51 does not have the ability to adjust the S(α,β) card for temperatures as it does for the TMP card discussed above. Therefore, additional studies are performed to show the impact of the S(α,β) card at the two available temperatures.

To determine the water temperature and density which result in the maximum reactivity, MCNP5-1.51 calculations are run using the bounding values. Additionally, S(α,β) calculations are performed for both upper and lower bounding S(α,β) values, if needed.

The studies mentioned above are performed for the following cases for the single cell MCNP5-1.51 SFP model (with periodic boundary conditions through the centerline of the surrounding water²):

² [REDACTED]

- Case 2.3.2.1 (reference case): Temperature of 39.2 °F (277.15 K) and a density of 1.0 g/cc are used to determine the reactivity at the low end of the temperature range. The S(α,β) card corresponds to a temperature of 68.81 °F (293.6 K).
- Case 2.3.2.2: Temperature of 150 °F (338.71 K) and a corresponding density of 0.98026 g/cc are used to determine the reactivity at the high end of the temperature range. The S(α,β) card corresponds to a temperature of 68.81 °F (293.6 K).
- Case 2.3.2.3: Temperature of 150 °F and a corresponding density of 0.98026 g/cc. The S(α,β) card corresponds to a temperature of 170.33 °F (350 K).

The bounding water temperature and density (the temperature and its corresponding density which result in the maximum reactivity) of the above cases are applied to all further calculations so that the most reactive water temperature and density is considered. Note that the evaluations use the same MCNP5-1.51 models used in the design basis calculation. [REDACTED]

2.3.3 Fuel Depletion Calculation Uncertainty

To account for the uncertainty of the number densities in the depletion calculations performed in CASMO-4, a 5% depletion uncertainty factor as described in [2] and [6] is used. [REDACTED]

The depletion uncertainty is applied by multiplying it with the reactivity difference (at 95%/95%) between the MCNP5-1.51 calculation with spent fuel at peak reactivity (includes residual Gd) and a corresponding MCNP5-1.51 calculation with fresh fuel (without Gd₂O₃). Calculations are performed for the single cell model of design basis fuel assembly.

The uncertainty is determined by the following:

$$\text{Uncertainty}_{\text{Isotopics}} = [(k_{\text{calc-2}} - k_{\text{calc-1}}) + 2 * \sqrt{(\sigma_{\text{calc-1}}^2 + \sigma_{\text{calc-2}}^2)}] * 0.05$$

with

$k_{\text{calc-1}}$ = k_{calc} with spent fuel

$k_{\text{calc-2}}$ = k_{calc} with fresh fuel

$\sigma_{\text{calc-1}}$ = Standard deviation of $k_{\text{calc-1}}$

$\sigma_{\text{calc-2}}$ = Standard deviation of $k_{\text{calc-2}}$

The result of the MCNP5-1.51 calculation for the fuel depletion calculation uncertainty is statistically combined with other uncertainties to determine k_{eff} .

2.3.4 Fuel and Storage Rack Manufacturing Tolerances

In order to determine the k_{eff} of the SFP at a 95% probability at a 95% confidence level, consideration is given to the effect of the BWR fuel and SFP storage rack manufacturing tolerances on reactivity. The reactivity effects of significant independent tolerance variations are combined statistically [2]. The evaluations use the same MCNP5-1.51 models used in the design basis calculation.

2.3.4.1 Fuel Manufacturing Tolerances

The BWR fuel tolerances for Optima2 QI22 fuel (which is the most reactive fuel design evaluated herein) are presented in Table 5.1(a). Fuel tolerance calculations are performed using the design basis fuel assembly lattice, and therefore only the tolerances applicable to that lattice are applicable. Separate CASMO-4 depletion calculations are performed for each fuel tolerance and the full value of the tolerance is applied for each case in both the depletion and in rack calculations. Pin specific compositions are used. The MCNP5-1.51 tolerance calculation is compared to the MCNP5-1.51 reference case (nominal parameter values) at the 95% probability at a 95% confidence level using the following equation:

$$\text{delta-}k_{\text{calc}} = (k_{\text{calc}2} - k_{\text{calc}1}) \pm 2 * \sqrt{(\sigma_1^2 + \sigma_2^2)}$$

The following fuel tolerances are considered in this analysis:

- Fuel enrichment
- Gd loading
- Fuel pellet density (UO₂ and UO₂+Gd₂O₃ fuel rods)
- Fuel pellet outer diameter (OD)
- Fuel cladding inner diameter (ID)
- Fuel cladding OD
- Fuel pin pitch
- Fuel sub-bundle pitch³
- Combination of⁴
 - Water wing canal inner width
 - Channel outer square width
 - Channel corner inner radius
 - Central water canal inner square width
- Combination of⁴
 - channel wall thickness

³ For fuel sub-bundle pitch uncertainty calculation, the fuel hardware (channel, central water channel and water wings) is fixed. The fuel lattices are moved only.

⁴ Conservatively, the various tolerances are considered together. The tolerance limits that result in an increase of the amount of water in the core are considered together in one set of uncertainty calculations, and the tolerance limits that result in a decrease of the amount of water in the core are considered together in another set of uncertainty calculations.

- Water cross wall thickness

The maximum positive reactivity effect of the MCNP5-1.51 calculations for each tolerance is statistically combined with the other tolerance results, and this result is then statistically combined with other uncertainties when determining the k_{eff} value.

2.3.4.2 SFP Storage Rack Manufacturing Tolerances

The SFP rack tolerances are presented in Tables 5.3(a) and 5.3(b). The single cell MCNP5-1.51 model is used to determine the reactivity effect of the tolerance, and the full value of the tolerance is applied for each case. The MCNP5-1.51 tolerance calculation is compared to the MCNP5-1.51 reference case with a 95% probability at a 95% confidence level using the following equation:

$$\text{delta-}k_{\text{calc}} = (k_{\text{calc}2} - k_{\text{calc}1}) \pm 2 * \sqrt{(\sigma_1^2 + \sigma_2^2)}$$

The following SFP rack manufacturing tolerances are considered in this analysis:

- Storage cells:
 - Cell ID and cell pitch
 - Cell wall thickness
- Rack inserts (poison)
 - Width

The maximum positive reactivity effect of the MCNP5-1.51 calculations for each tolerance is statistically combined with the other tolerance results, and this result is then statistically combined with other uncertainties when determining the k_{eff} value.

The evaluations use the same MCNP5-1.51 models used in the design basis calculation. The isotopic compositions of the fuel rods are the same as those of the design basis fuel assembly.

The poison thickness and loading are used at their minimum values; i.e., they are treated as a bias instead of uncertainty, for conservatism and simplification.

2.3.5 Radial Positioning

2.3.5.1 Fuel Assembly Orientation in the Core

The fuel assembly orientation in the core with respect to its control blade does not change and therefore the design basis calculations consider the only possible configuration.

2.3.5.2 Fuel Radial Positioning in the Rack

The BWR fuel that is loaded in the SFP racks may not rest exactly in the center of the storage cell. Evaluations are performed to determine the most limiting fuel radial location. The following eccentric fuel positioning cases are analyzed:

- Case 2.3.5.2.1: This is the reference for Case 2.3.5.2.2 through Case 2.3.5.2.5. The MCNP5-1.51 model used herein is a 2x2 array which is the same as the primary single bundle MCNP5-1.51 model used elsewhere in this analysis. In both models the fuel is centered in the rack cell. See Figure 2.7(a).
- Case 2.3.5.2.2: Every fuel assembly is positioned toward the center, for the 2x2 array, as shown in Figure 2.7(b).
- Case 2.3.5.2.3: Every fuel assembly is positioned toward the corner where the insert wings connect, for the 2x2 array, as shown in Figure 2.7(c).
- Case 2.3.5.2.4: Every fuel assembly is positioned away from the corner where the insert wings connect, for the 2x2 array, as shown in Figure 2.7(d).
- Case 2.3.5.2.5: Every fuel assembly is centered between insert and cell walls, for the 2x2 array, as shown in Figure 2.7(e).
- Case 2.3.5.2.6: This is the reference for Case 2.3.5.2.7 through Case 2.3.5.2.10. The MCNP5-1.51 model used herein is an 8x8 array which is the same as the primary single bundle MCNP5-1.51 model used elsewhere in this analysis. In both models the fuel is centered in the rack cell.
- Case 2.3.5.2.7: Every fuel assembly is positioned toward the center, for the 8x8 array, as shown in Figure 2.8.
- Case 2.3.5.2.8: Every fuel assembly is positioned toward the corner where the insert wings connect, for the 8x8 array.
- Case 2.3.5.2.9: Every fuel assembly is positioned away from the corner where the insert wings connect, for the 8x8 array.
- Case 2.3.5.2.10: Every fuel assembly is centered between insert and cell walls, for the 8x8 array.
- Case 2.3.5.2.11: This is the reference for Case 2.3.5.2.12. The MCNP5-1.51 model used herein is a single rack cell where the fuel is centered.
- Case 2.3.5.2.12: The fuel assembly is centered between insert and cell walls, for the single rack cell.

The maximum positive reactivity effect of the MCNP5-1.51 calculations for the fuel radial positioning is added as the bias and the corresponding 95/95 uncertainty is statistically combined with other uncertainties to determine k_{eff} .

Note that the evaluations use the same MCNP5-1.51 models with periodic boundary conditions used in the design basis calculation, except that the array size is larger. The isotopic compositions of the fuel rods are the same as those of the design basis fuel assembly.

2.3.5.3 Inserts Radial Positioning

Since the insert width and SFR cell inner diameter are comparable, and each insert is installed into the rack cell such that the insert becomes an integral part of the fuel rack, no uncertainty in the positioning for inserts is evaluated. The water gap between rack wall and insert is not assumed, since it may provide a small flux trap effect. Nevertheless, the orientation of fuel assembly with respect to position of insert is considered in Section 2.3.5.4.

2.3.5.4 Fuel Orientation in SFP Rack Cell

As described in Section 5.1, fuel assemblies have various radial fuel enrichments and gadolinium distribution. Also, one corner of each fuel assembly is adjacent to the control blade during the depletion in the core. As a result, the fuel depletion is not uniform (more discussion is provided in Section 2.3.1.1.2) and one fuel assembly corner may be more reactive than other corners and therefore the fuel assembly orientation in the SFP storage cell may have an impact on reactivity.

Five cases are analyzed to assess the fuel assembly orientation variations and to determine the most limiting fuel orientation in SFP rack cell with respect to the insert.

The MCNP5-1.51 model of the reference case is the design basis fuel in the 2x2 array, as shown in Figure 2.9(a). The MCNP5.1.51 models of the other four cases are the same as that of the reference case, except with different orientation of fuel assemblies with respect to the inserts. Figure 2.9(b) through Figure 2.9(e) show the configurations of the fuel assemblies in the SFP cells for the evaluated cases.

Note that the evaluations use the same MCNP5-1.51 models with periodic boundary conditions used in the design basis calculation. The isotopic compositions of the fuel rods are the same as those of the design basis fuel assembly.

2.3.6



2.3.6.1 [REDACTED]

[REDACTED]

2.3.6.1.1 [REDACTED]

2.3.6.1.2 [REDACTED]

[REDACTED]

2.3.6.2 [REDACTED]

[REDACTED]

[REDACTED]

2.3.7 Insert Coupon Measurement Uncertainty

There is a measurement uncertainty associated with the B-10 content in the poison test coupons. In this analysis, the minimum B-10 loading and the minimum insert thickness are conservatively used for criticality calculations. Therefore, the coupon measurement uncertainty is not evaluated further in the analysis.

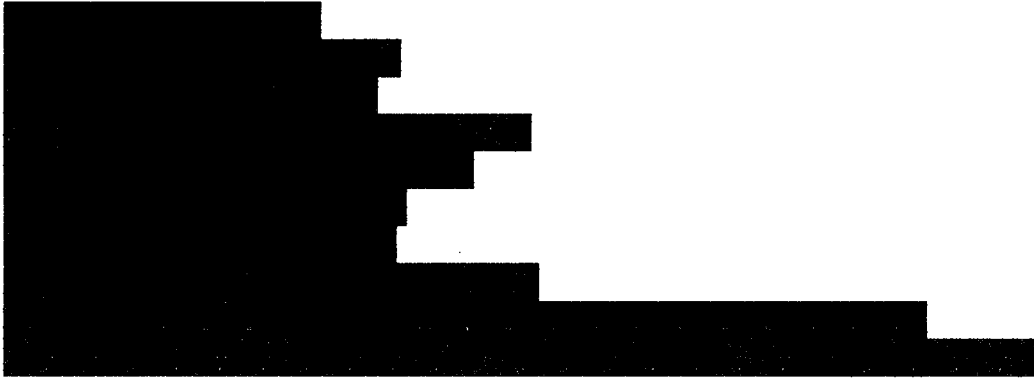
2.3.8 Maximum k_{eff} Calculation for Normal Conditions

The calculation of the maximum k_{eff} of the SFP storage racks fully loaded with design basis fuel assemblies at their maximum reactivity is determined by adding all uncertainties and biases to the calculated reactivity. Note that the insert thickness and its B-10 loading are taken at their worst case values.

k_{eff} is determined by the following equation:

$$k_{eff} = k_{calc} + \text{uncertainty} + \text{bias}$$

where uncertainty includes:



and the bias includes



Note that each uncertainty is statistically combined with other uncertainties, while biases are added together in order to determine k_{eff} .

The approach used in this analysis takes credit for residual Gd.

2.4 Margin Evaluation

The criticality analysis is performed using several conservative assumptions which introduce quantifiable margin into the analysis. Four main conservative assumptions are:

- Minimum insert B₄C loading
- Minimum insert thickness
- Minimum amount of B-10 in boron
- Bounding lattice throughout the entire length of fuel assembly.

To evaluate this margin, the following cases are evaluated:

- Case 2.4.1: This is the design basis fuel assembly. This is the reference for Case 2.4.2 and Case 2.4.3.

- Case 2.4.2: This case is the same as Case 2.4.1, except the nominal insert B₄C loading, nominal insert thickness and nominal amount of B-10 in boron are used.
- Case 2.4.3: This case is the same as Case 2.4.1, except the model includes each Optima2 QI22 fuel lattice in the appropriate axial position. However, the top and bottom blankets were conservatively replaced by adjacent fuel lattices. The peak reactivity burnup for each individual Optima2 QI22 lattice under the design basis core operation parameters was determined separately and used in this case (i.e. each lattice is at its individual peak reactivity). Therefore, the model represents a conservative maximum but unrealistic reactivity of the actual Optima2 fuel assembly.

The differences between the reactivity of Cases 2.4.2 and 2.4.3 and the reactivity of reference Case 2.4.1 provide a quantified margin.

Note that the evaluations use the same MCNP5-1.51 models used in the design basis calculation. The isotopic compositions of the fuel rods of Case 2.4.1 and Case 2.4.2 are the same as those of the design basis fuel assembly.

2.5 Fuel Movement, Inspection and Reconstitution Operations



2.6 Accident Condition

The accidents considered are:

- SFP temperature exceeding the normal range
- Dropped assemblies
- Storage cell distortion
- Missing insert
- Misloaded fuel assembly (a fuel assembly in the wrong location within the storage rack)/
Missing an insert
- Mislocated fuel assembly (a fuel assembly in the wrong location outside the storage rack)
- Miss-installment of an insert on wrong sides of a cell
- Insert mechanical wear
- Rack movement

Those are briefly discussed in the following sections.

Note that the double contingency principle as stated in [2] specifies that “two unlikely independent and concurrent incidents or postulated accidents are beyond the scope of the required analysis.” This principle precludes the necessity of considering the simultaneous occurrence of multiple accident conditions. The k_{eff} calculations performed for the accident conditions are done with a 95% probability at a 95% confidence level.

The accident conditions are considered at the 95/95 level using the total corrections from the design basis case. [REDACTED]

2.6.1 Temperature and Water Density Effects

The SFP water temperature accident conditions for consideration are the increase in SFP water temperature above the maximum SFP operating temperature of 150 °F. The decrease in temperature was already considered for the temperature coefficient determination as discussed in Section 2.3.2. To bound the potential increase in reactivity due to increased SFP temperature, the following case is evaluated:

- Case 2.6.1: This case uses a temperature of 255 °F (397.04 K) and a density of 0.84591 g/cc. The $S(\alpha,\beta)$ card corresponds to a temperature of 260.33 °F (400 K). In this model, it is assumed that the water modeled includes 10% void. Void is modeled as 10% decrease in density, compared to the density of water at 255 °F.

The evaluation use the same MCNP5-1.51 model used in the design basis calculation.

Note that as discussed in Section 2.3.2, SFP storage racks with strong neutron absorbers, such as inserts, show a higher reactivity at a lower water temperature. The case evaluated above is performed to confirm this statement.

2.6.2 Dropped Assembly – Horizontal

For the case in which a fuel assembly is assumed to be dropped on top of a rack, the fuel assembly will come to rest horizontally on top of the rack with a separation distance more than 12 inches. Also, the length of the inserts (as indicated in Table 5.3(b)) covers this separation distance. Thus, the horizontally dropped assembly is decoupled from the fuel assemblies in the rack. This accident is also bounded by the mislocated case, where the mislocated assembly is closer to the assembly in the racks. Therefore, the horizontally dropped fuel assembly is not evaluated further in the report.

2.6.3 Dropped Assembly – Vertical into a Storage Cell

It is also possible to vertically drop an assembly into a location that might be occupied by another assembly or that might be empty. Such a vertical impact would at most cause a small compression of the stored assembly, if present, or result in a small deformation of the baseplate for an empty cell.

These deformations could potentially increase reactivity. However, the reactivity increase would be small compared to the reactivity increase created by the 'misloaded fuel assembly/missing insert' accident (discussed in Section 2.6.5) that does not include the insert in one rack cell. The vertical drop is therefore bounded by this misload accident and no separate calculation is performed for this drop accident.

2.6.4 Storage Cell Distortion

A storage cell distortion or altered geometry as a result of fuel handling equipment uplift forces is possible. However, the reactivity increase would be small compared to the possible reactivity increase created by the 'misloaded fuel assembly/missing insert' accident that does not include the insert in one rack cell, as discussed in Section 2.6.5. The storage cell distortion is therefore bounded by the 'misloaded fuel assembly/missing insert' accident and no separate calculation is performed for the storage cell distortion accident.

As a result of significant distortion, the storage cell for whatever reason may not be able to contain the insert and also it will be therefore unacceptable for storage of a fuel assembly. This condition is bounded by the 'misloaded fuel assembly/missing insert' accident. However to show that it is acceptable for normal operation and that the empty storage cell decreases the reactivity of the SFR, the model with an empty storage cell, i.e. without a fuel assembly and insert, in the center of a 8x8 array, is evaluated. Two cases with a cell centered and eccentric position of the fuel assemblies are analyzed.

2.6.5 Misloaded Fuel Assembly/Missing Insert

The fuel storage racks are qualified for storage of fuel assembly with the highest anticipated reactivity; thus it is not possible to misload a fuel assembly if every cell with a fuel assembly has an insert.

However, there are a few cells in the SFP racks which are exempt from fuel storage. Those locations are blocked or have partial interferences. In a hypothetical scenario, it is assumed that a fuel assembly is misloaded into a cell with a missing insert. To evaluate the effect, the following cases are evaluated:

- Case 2.6.5.1: The MCNP5-1.51 model includes an 8x8 array. One cell near the center of the rack does not have the insert. The misloaded fuel assembly is the design basis fuel assembly. This fuel assembly is eccentric toward the walls that are not covered by inserts. Other fuel assemblies are also eccentric toward the misloaded fuel assembly. The periodic boundary conditions are used through the centerline of the surrounding water (BORAFLEX replacement). The temperature of the model is set to the minimum (39.2 °F) with its corresponding water density and S(α,β) card. These temperature and density are bounding for the SFP racks. See Figure 2.10(a).
- Case 2.6.5.2: The MCNP5-1.51 model is the same as Case 2.6.5.1, except with all fuel assemblies centered in the rack cells. See Figure 2.10(b).

2.6.6 Mislocated Fuel Assembly

The Quad Cities SFP layout was reviewed to determine the possible worst case locations for a mislocated fuel assembly. Three hypothetical locations where a fuel assembly may be mislocated are:

- In the water gap between the racks and the pool wall
- In the corner between two racks
- Between the SFP rack and the inspection platform.

The three cited scenarios are evaluated, as follows.

2.6.6.1 Mislocation of a Fuel Assembly in the Water Gap between the Racks and Pool Wall

A fuel assembly may be mislocated in the water gap between the racks and the pool wall. Due to the neutron leakage to the outside the storage rack area, the effect of this mislocation is bounded by that of 'mislocation of a fuel assembly between the SFP rack and the inspection platform' accident, as discussed in Section 2.6.6.3. No separate calculation is performed for this accident.

2.6.6.2 Mislocation of a Fuel Assembly in the Corner between Two Racks

There are some places in the SFP, but outside of the racks, where the mislocated fuel assembly may be in the corner between two racks (thus the mislocated fuel assembly would be adjacent to the fuel assemblies in racks from two sides). To evaluate the effect of the mislocation of a fuel assembly in the corner between two racks, the following cases are evaluated:

- Case 2.6.6.2.1: The MCNP5-1.51 model is three 8x8 arrays of SFP rack cells. The misplaced fuel assembly is in the corner between two racks. The fuel assemblies in the rack are eccentric toward the mislocated fuel assembly. The misplaced fuel assembly is placed as close to the racks as possible. All fuel assemblies in the model are the design basis fuel assembly. Figures 2.11(a) and 2.11(b) show the MCNP5-1.51 model used for this analysis.
- Case 2.6.6.2.2: The MCNP5-1.51 model is the same as Case 2.6.6.2.1, except with all fuel assemblies are centered. See Figures 2.11(a) and 2.11(c).
- Case 2.6.6.2.3: The MCNP5-1.51 model is the same as Case 2.6.6.2.1, except the temperature of the model is set to the maximum (150 °F).
- Case 2.6.6.2.4: The MCNP5-1.51 model is the same as Case 2.6.6.2.2, except the temperature of the model is set to the maximum (150 °F).

2.6.6.3 Mislocation of a Fuel Assembly between the SFP Rack and the Inspection Platform

As discussed in Section 2.5, the fuel handling/inspection/reconstitution platform may have one fuel assembly in it at a time. There is a possibility that a fuel assembly is mislocated between the

SFP racks and the fuel assembly in the platform. To evaluate the effect of the mislocation of a fuel assembly between the SFP Rack and the Inspection Platform, the following cases are evaluated:

- Case 2.6.6.3.1: The MCNP5-1.51 model is an 8x8 array of SFP rack cells. The misplaced fuel assembly is adjacent to the SFP rack and the inspection platform. The fuel assembly in the platform is lined up with the mislocated fuel assembly. The fuel assemblies in the rack are eccentric toward the mislocated fuel assembly: The misplaced fuel assembly is placed as close to the rack and fuel assembly in the inspection station as possible. All fuel assemblies in the model are design basis fuel assembly. The side of the fuel in the platform which does not have any fuel has at least 12 inches of water. Figure 2.12(a) shows the MCNP5-1.51 model used for this analysis.
- Case 2.6.6.3.2: The MCNP5-1.51 model is the same as Case 2.6.6.3.1, except with all fuel assemblies are centered. See Figure 2.12(b).
- Case 2.6.6.3.3: The MCNP5-1.51 model is the same as Case 2.6.6.3.1, except the temperature of the model is set to the maximum (150 °F).
- Case 2.6.6.3.4: The MCNP5-1.51 model is the same as Case 2.6.6.3.2, except the temperature of the model is set to the maximum (150 °F).

2.6.7 Mis-installment of an Insert on Wrong Side of a Cell

There is a small possibility that an insert is installed on wrong sides of the cell. In this case, there may not be a poison between a fuel assembly placed in that cell and a fuel assembly in an adjacent cell. However, the effect of this mis-installment is bounded by that of ‘misloaded fuel assembly/missing insert’ accident that does not include the insert in one rack cell, as discussed in Section 2.6.5. No separate calculation is performed for this accident.

2.6.8 Insert Mechanical Wear

Handling accidents and other environmental damage may cause scratches and local wear of inserts. The effect of this accident is bounded by that of ‘misloaded fuel assembly/missing insert’ accident, as discussed in Section 2.6.5.

2.6.9 Rack Movement

In the event of seismic activity, there is a hypothetical possibility that the storage rack arrays may move and come closer to each other. Since there is no water gap modeled between cells of a storage rack, the reactivity of the rack movement case is bounded by the reactivity of the design basis calculation.

2.7 [REDACTED]

2.7.1 [Redacted]

[Redacted]

[Redacted]

[Redacted]

[Redacted]

- [REDACTED]
 - [REDACTED]
 - [REDACTED]
- [REDACTED]
 - [REDACTED]



2.8 Spent Fuel Rack Interfaces

The spent fuel pool includes a single type of Region 1 spent fuel racks, which are loaded with the neutron absorbing inserts in every storage cell as well as a uniform fuel assembly loading pattern. Therefore, any possible water gaps and interfaces between the racks are bounded by the infinite array used in the design basis calculations. However, since the neutron absorbing inserts are located in the same corners of rack cells (e.g. south-west), there are two peripheral rows of the cells (correspondingly, north and east periphery of the pool), which are loaded with the fuel assemblies that have one side that is not adjacent to the insert. Furthermore, one fuel assembly in the corner of the spent fuel pool (correspondingly, north-east corner) has two sides that are not adjacent to the insert. Due to the neutron leakage on the periphery of the spent fuel pool the reactivity increase is not expected. Nevertheless, to evaluate the effect of such conditions, the full spent fuel pool model (74x74 array) loaded with the cell centered design basis fuel assemblies and the model where all fuel assemblies are shifted to the fuel assembly in the corner, which is discussed above, were evaluated.

2.9 Reconstituted Fuel Assemblies

The SFP contains various reconstituted assemblies which were examined and determined to be relatively old and low reactivity designs. The reconstitution of these fuel assemblies removed fuel rods and replaced them by either fuel rods that are of the same or less initial enrichment and equal or greater Gd loading (with burnup similar to the rod they replaced) or solid stainless steel rods. The reactivity effect of this reconstitution is not sufficient to make the reconstituted fuel assembly more reactive than the bounding lattice. Therefore, reconstituted assemblies are covered by the design basis Optima2 QI22 lattice 146. Future reconstituted assemblies will replace fuel rods with stainless steel rods.

3. ACCEPTANCE CRITERIA

3.1 *Applicable Codes, Standards and Guidance's*

Codes, standard, and regulations or pertinent sections thereof that are applicable to these analyses include the following:

- Code of Federal Regulations, Title 10, Part 50, Appendix A, General Design Criterion 62, "Prevention of Criticality in Fuel Storage and Handling."
- Code of Federal Regulations, Title 10, Part 50.68, "Criticality Accident Requirements."
- USNRC Standard Review Plan, NUREG-0800, Section 9.1.1, Criticality Safety of Fresh and Spent Fuel Storage and Handling, Revision 3 – March 2007.
- L. Kopp, "Guidance on the Regulatory Requirements for Criticality Analysis of Fuel Storage at Light-Water Reactor Power Plants," NRC Memorandum from L. Kopp to T. Collins, August 19, 1998.
- ANSI ANS-8.17-1984, Criticality Safety Criteria for the Handling, Storage and Transportation of LWR Fuel Outside Reactors (withdrawn in 2004).
- USNRC, NUREG/CR-6698, Guide for Validation of Nuclear Criticality Safety Calculational Methodology, January 2001.
- DSS-ISG-2010-01, Revision 0, Staff Guidance Regarding the Nuclear Criticality Safety Analysis for Spent Fuel Pools.

4. ASSUMPTIONS

The analyses apply a number of assumptions, either for conservatism or to simplify the calculation approach. Important aspects of applying those assumptions are as follows:

1. Bounding or sufficiently conservative inputs and assumptions are used essentially throughout the entire analyses, and as necessary studies are presented to show that the selected inputs and parameters are in fact conservative or bounding.
2. Neutron absorption in minor structural members of the fuel assembly is neglected, e.g., spacer grids are replaced by water. It is conservative to neglect the spacer grids because this spent fuel pool contains no soluble boron, the region around the fuel rods is under-moderated, as confirmed by the fuel tolerances calculations that change the fuel to moderator ratio (Section 7.1.7.1); therefore, neglecting the spacer grid places more water within the calculation model. In addition, the inconel springs within the spacer are a stronger neutron absorber than water. The active fuel region repeats periodically in the vertical direction. Therefore, neutron absorption in upper and lower tie plates, fuel plenums, etc. is neglected.
3. The neutron absorber length in the rack is more than the active region of the fuel, but it is modeled to be the same length.
4. The fuel density is assumed to be equal to the pellet density, and is conservatively modeled as a solid right cylinder over the entire active length, neglecting dishing and chamfering. This is acceptable since the amount of fuel modeled is more than the actual amount.
5. For the inserts, only the worst case bounding material specifications are used (minimum B-10 loading and minimum thickness).
6. All models are laterally infinite arrays of the respective configuration, neglecting lateral leakage. The exception is where the model boundaries are water, as specified.
7. All fuel cladding materials are modeled as pure zirconium, while the actual fuel cladding consists of one of several zirconium alloys. This is acceptable since the model neglects the trace elements in the alloy which provide additional neutron absorption.
8. 
9. The full spent fuel pool model is considered as a 74x74 array of storage cells. The water gaps between the spent fuel racks were conservatively neglected.

5. INPUT DATA

5.1 Fuel Assembly Specification

The SFP racks are designed to accommodate the following fuel assembly types used in the Quad Cities Unit 1 and Unit 2, which are presented in a chronologic order along with the initial maximum planar average enrichment (IMPAAE):

- [REDACTED]

The specifications for the most reactive fuel assemblies from the fuel product lines discussed above are presented in Table 5.1. The additional specifications for other fuel design variations are presented in Appendix A.

The fuel assembly MCNP model used for the design basis calculations is presented in Figure 5.4. The fuel rod, cladding and channel are explicitly modeled. [REDACTED]

[REDACTED] Axially, the design basis MCNP model considers the bounding lattice along the entire length and uses water reflectors at the top and bottom. The MCNP model for the margin evaluation calculations discussed in Section 2.4 differ from the design basis model in that the active length specifically considers each actual lattice in its actual axial configuration (i.e. all the lattices from the Q122 bundle are modeled in the same MCNP model). [REDACTED]

5.2 Reactor Parameters

The reactor core parameters are provided in Table 5.2(a). The reactor control blade data are provided in Table 5.2(b). The reactor control parameters used in CASMO-4 screening and design basis calculations are provided in Table 5.2(c).

5.3 Spent Fuel Pool Parameters

The spent fuel pool parameters are provided in Table 5.2(a).

5.4 Storage Rack Specification

The storage rack specifications that are used in the criticality analysis are summarized in Tables 5.3(a) and 5.3(b). The Quad Cities Unit 1 and Unit 2 SFP are shown in Figures 5.2(a) and 5.2(b), respectively.



The MCNP5-1.51 SFP model consists of a single rack cell with periodic boundary conditions through the centerline of the water (BORAFLEX replacement), thus simulating an infinite array of storage cells. The storage rack cell is modeled the same length as the active fuel and all other storage rack materials are neglected. The neutron absorber is modeled with the worst case bounding values (the minimum B-10 loading and the minimum thickness) provided in Table 5.3(b) and Figure 5.3. The cell wall thickness of the boundary is different from that of inner walls. The cell wall thickness of the boundary is thicker than the inner wall thickness. The SFP model uses the inner cell wall thickness only, as given in Table 5.3(a), because it decreases the amount of steel in the model, which acts a neutron absorber.

The MCNP5-1.51 SFP rack cell model is shown in Figure 5.4.

5.4.1 Material Compositions

The MCNP5-1.51 material specification is provided in Table 5.4(a) for non-fuel materials, and in Table 5.4(b) for fuel materials.

6. COMPUTER CODES

The following computer codes were used in this analysis.

- MCNP5-1.51 [1] is a three-dimensional continuous energy Monte Carlo code developed at Los Alamos National Laboratory. This code offers the capability of performing full three dimensional calculations for the loaded storage racks. MCNP5-1.51 was run on the PCs at Holtec.
- CASMO-4 [4] is a two-dimensional multigroup transport theory code developed by Studsvik. CASMO-4 is used to perform the depletion calculation for the pin-specific approach, and for various studies. CASMO-4 was run on the PCs at Holtec.

7. ANALYSIS

7.1 *Design Basis and Uncertainty Evaluations*

7.1.1 [REDACTED]



7.1.2 **Determination of the Design Basis Fuel Assembly Lattice**

As discussed in Section 2.3.1.3, MCNP5-1.51 calculations were performed to determine the design basis lattice. The results for the SVEA-96 Optima2 QI22 fuel assembly are presented in Table 7.2(a). The results for the GE14 lattice type 5 are presented in Table 7.2(b), along with the bounding result of the SVEA-96 Optima2 QI22. As can be seen, the SVEA-96 Optima2 QI22 lattice type 146 is bounding, and thus it is selected as the design basis lattice. The CASMO-4 model of the SVEA-96 Optima2 bundle QI22 lattice 146 used for depletion calculations is shown in Figure 5.1.

7.1.2.1 Fuel Assembly De-Channeling

As discussed in Section 2.3.1.5.4, the reactivity of the second most reactive assembly with no Zr channel at various radial positioning was evaluated. The results are provided in Table 7.2(b) and compared with the reactivity of the design basis lattice (SVEA-96 Optima2 QI22 lattice type 146). As can be seen, the SVEA-96 Optima2 QI22 lattice type 146 is bounding. Therefore, storage of fuel assemblies without channels is acceptable.

7.1.3 **Optima2 CASMO-4 Model Simplification Effect**

As discussed in Section 2.3.1.4, the effect of CASMO-4 model simplifications on the calculated reactivity of the SVEA-96 Optima2 QI22 lattice 146 was evaluated. The results are provided in Table 7.3. As can be seen, the reactivity of the simplified model is comparable to that of the complete model of SVEA-96 Optima2 QI22 lattice 146 (essentially within the 95/95 uncertainty between the two calculations). Therefore, the results show that the CASMO-4 model simplification

does not have a significant impact on the analysis conclusions regarding the determination of the design basis lattice.

7.1.4 Core Operating Parameters

As discussed in Section 2.3.1.5, the effects of the core operating parameters on the reactivity were evaluated. The results are provided in Table 7.4. The results show that the two dominant core operating parameters are the control blade insertion and void fraction. The other core operating parameters have an insignificant impact. Therefore, the design basis (bounding) core operating parameters are: control blades inserted, 0% void fraction, maximum fuel and moderator temperature and maximum specific power.

7.1.4.1 Reactor Power Uprate

As discussed in Section 2.3.1.5.1, the effect of the MUR on the reactivity was evaluated. The results are provided in Table 7.4. The most important core operating parameters are rodged operation (control blades) and void fraction. Other parameters have relatively negligible effects on reactivity. As can be seen, the calculations with the increased power density show statistically equivalent results, which confirms the negligible effect of the reactor power uprate on reactivity.

7.1.5 Water Temperature and Density Effect

As discussed in Section 2.3.2, the effects of water temperature, and the corresponding water density and temperature adjustments ($S(\alpha,\beta)$) were evaluated for SFP racks. The results of these calculations are presented in Table 7.5.

The results of the SFP temperature and density calculations show that as expected (for poisoned racks) the most reactive water temperature and density for the SFP racks is a temperature of 39.2 °F at a density of 1 g/cc, and these values are used for all calculations in SFP racks.

7.1.6 Depletion Uncertainty

As discussed in Section 2.3.3, the uncertainty of the number densities in the depletion calculations was evaluated. The results of these calculations are presented in Table 7.6(a).

Also, as discussed in Section 2.2.1.1.1, the uncertainty associated with FPs and LFPs was evaluated. The results of these calculations are presented in Table 7.6(b).

These two uncertainties are statistically combined with other uncertainties to determine k_{eff} in Table 7.11 and Table 7.14.

7.1.7 Fuel and Rack Manufacturing Tolerances

7.1.7.1 Fuel Assembly Tolerances

As discussed in Section 2.3.4.1, the effect of the BWR fuel tolerances on reactivity was determined. The results of these calculations are presented in Table 7.7. The maximum positive delta-k value for each tolerance is statistically combined.

The maximum statistical combination of fuel assembly tolerances is used to determine k_{eff} in Table 7.11 and Table 7.14.

7.1.7.2 SFP Rack Tolerances

As discussed in Section 2.3.4.2, the effect of the manufacturing tolerances on reactivity of the SFP racks with inserts was determined. The results of these calculations are presented in Table 7.8. The maximum positive delta-k value for each tolerance is statistically combined.

The maximum statistical combination of the SFP rack tolerances is used to determine k_{eff} in Table 7.11 and Table 7.14.

7.1.8 Radial Positioning

7.1.8.1 Fuel Assembly Radial Positioning in SFP Rack

As discussed in Section 2.3.5.2, twelve fuel assembly radial positioning cases in racks were evaluated. The results of these calculations are presented in Table 7.9(a). For each eccentric position case, the result for similar but cell centered case is considered as a reference. The results show that most cases show a negative reactivity effect, however some delta k_{calc} values are positive. Therefore, a maximum delta k_{calc} value is applied as a bias and the correspondent 95/95 uncertainty is statistically combined with other uncertainties in Table 7.11 and Table 7.14.

7.1.8.2 Fuel Orientation in SFP Rack

As discussed in Section 2.3.5.4, five fuel assembly orientation cases in racks were evaluated. The results of these calculations are presented in Table 7.9(b). The result for the reference case is also included. The results show that all cases are statistically equivalent and the reactivity effect of fuel orientation is negligible. Nevertheless, a maximum positive delta k_{calc} value is applied as a bias and the correspondent 95/95 uncertainty is statistically combined with other uncertainties in Table 7.11 and Table 7.14.

7.1.9 Fuel Rod Geometry Change

7.1.9.1 [REDACTED]

[REDACTED] The results are presented in Table 7.10.

The maximum ' $k_{\text{calc}} - k_{\text{calc,reference}}$ ' is added as a bias, and the ' $2 * \sqrt{(\sigma_{\text{calc}}^2 + \sigma_{\text{calc,reference}}^2)}$ ' (95/95 uncertainty) is added as an uncertainty to determine k_{eff} in Table 7.11 and Table 7.14.

7.1.9.2 [REDACTED]

7.1.10 [REDACTED]

7.2 Maximum k_{eff} Calculations for Normal Conditions

As discussed in Section 2.3.8, the maximum k_{eff} for normal conditions is calculated. The results are tabulated in Table 7.11. The results show that the maximum k_{eff} for the normal conditions in the SFP racks is less than 0.95 at a 95% probability and at a 95% confidence level.

7.3 Margin Evaluation

As discussed in Section 2.4, the margin analyses were performed using the nominal values for poison thickness and loading, as well as the actual lattice configuration of the Optima2 QI22 fuel assembly. The results of calculations are provided in Table 7.12(a) and Table 7.12(b). As can be seen and is expected, the reactivity of design basis is larger. The use of a minimum B-10 loading relative to use of a nominal B-10 loading with tolerance uncertainty provide an additional ~1% reactivity margin to the regulatory limit with a 95% probability at a 95% confidence level.

The summary of the margin evaluation is presented in Table 7.12(c). The result shows that quantified margin remains in the analysis to offset potential effects not already considered in the model.

7.4 *Abnormal and Accident Conditions*

As discussed in Section 2.6, the effects of empty storage cell, increased temperature, misloaded fuel assembly/missing insert, and mislocated fuel assembly accidents on reactivity were evaluated. The results are provided in Table 7.13(a) and Table 7.13(b).

As can be seen, the increased water temperature will not result in an increase in reactivity.

Both misloaded fuel assembly/missing insert and mislocated fuel accidents may result in an increase in reactivity. For the SFP racks, the effect on reactivity of the missing insert is the limiting case. Thus, its calculated MCNP5-1.51 k_{calc} is used for maximum k_{eff} calculations for abnormal and accident conditions, discussed in Section 7.5 .

The condition with the empty storage cell without insert in the spent fuel rack shows a lower reactivity than a design basis case, therefore, it is acceptable to have the empty storage cell without insert in the spent fuel pool.

7.5 *Maximum k_{eff} Calculations for Abnormal and Accident Conditions*

As discussed in Section 2.6, the maximum k_{eff} for abnormal and accident conditions is calculated. The results are tabulated in Table 7.14. The results show that the maximum k_{eff} for abnormal and accident conditions in the SFP racks is less than 0.95 at a 95% probability and at a 95% confidence level.

7.6 [REDACTED]

[REDACTED]

[REDACTED]

7.7 Spent Fuel Rack Interfaces

As discussed in Sections 2.8, the interface between SFRs and pool walls, i.e. effect on reactivity of the peripheral fuel assemblies, that have a side non-adjacent to the insert, was evaluated. The results are provided in Table 7.17. As can be seen, this condition will not result in an increase of SFR reactivity. This result is expected because the infinite array design basis model is an infinite array of storage cells with inserts while the full pool model used for these rack interface calculations includes the rack edge along the pool wall where there is no insert along the water gap edge (i.e. no additional cell with an insert). Therefore, this water gap edge allows for neutron leakage and as the calculations show result in statistically equivalent results.

8. CONCLUSION

The criticality analysis for the storage of BWR assemblies in the Quad Cities SFP racks with NETCO-SNAP-IN[®] inserts has been performed. The results for the normal condition show that k_{eff} is [REDACTED] with the storage racks fully loaded with fuel of the highest anticipated reactivity, which is SVEA-96 Optima2 QI22 lattice type 146, at a temperature corresponding to the highest reactivity. The results for the accident condition show that k_{eff} is [REDACTED] with the storage racks fully loaded with fuel of the highest anticipated reactivity, which is SVEA-96 Optima2 [REDACTED] [REDACTED], at a temperature corresponding to the highest reactivity. The maximum calculated reactivity for both normal and accident conditions includes a margin for uncertainty in reactivity calculations with a 95% probability at a 95% confidence level. Reactivity effects of abnormal and accident conditions have been evaluated to assure that under all credible abnormal and accident conditions, the reactivity will not exceed the regulatory limit of 0.95.

[REDACTED]

[REDACTED]

[REDACTED]

[REDACTED]

[REDACTED]

[REDACTED]

9. REFERENCES

- [1] "MCNP - A General Monte Carlo N-Particle Transport Code, Version 5," Los Alamos National Laboratory, LA-UR-03-1987, April 24, 2003 (Revised 2/1/2008).
- [2] L.I. Kopp, "Guidance on the Regulatory Requirements for Criticality Analysis of Fuel Storage at Light-Water Reactor Power Plants," NRC Memorandum from L. Kopp to T. Collins, August 19, 1998.
- [3] "Nuclear Group Computer Code Benchmark Calculations," Holtec Report HI-2104790 Revision 1.
- [4] M. Edenius, K. Ekberg, B.H. Forssén, and D. Knott, "CASMO-4 A Fuel Assembly Burnup Program User's Manual," Studsvik/SOA-95/1; and J. Rhodes, K Smith, "CASMO-4 A Fuel Assembly Burnup Program User's Manual," SSP-01/400, Revision 5, Studsvik of America, Inc. and Studsvik Core Analysis AB (proprietary).
- [5] D. Knott, "CASMO-4 Benchmark Against Critical Experiments," SOA-94/13, Studsvik of America, Inc., (proprietary); and D. Knott, "CASMO-4 Benchmark Against MCNP," SOA-94/12, Studsvik of America, Inc., (proprietary).
- [6] DSS-ISG-2010-01, Staff Guidance Regarding the Nuclear Criticality Safety Analysis for Spent Fuel Pools, Revision 0.
- [7] Guide for Validation of Nuclear Criticality Safety Computational Methodology, NUREG/CR-6698, January 2001.
- [8] HI-2002444, Latest Revision, "Final Safety Analysis Report for the HI-STORM 100 Cask System", USNRC Docket 72-1014.
- [9] "Sensitivity Studies to Support Criticality Analysis Methodology," HI-2104598 Rev. 1, October 2010.
- [10] "Atlas of Neutron Resonances", S.F. Mughabghab, 5th Edition, National Nuclear Data Center, Brookhaven National Laboratory, Upton, USA.
- [11] "Spent Nuclear Fuel Burnup Credit Analysis Validation", ORNL Presentation to NRC, September 21, 2010.
- [12] An Approach for Validating Actinide and Fission Product Burnup Credit Criticality Safety Analyses—Criticality (k_{eff}) Predictions, NUREG/CR-7109, April 2012.
- [13] OECD / NEA Data Bank, Java-based Nuclear Information Software, Janis version 3.3 .

- [14] EPRI 1003222, "Poolside Examination Results and Assessment, GE11 BWR Fuel Exposed to 52 to 65 GWd/MTU at the Limerick 1 and 2 Reactors," December 2002.

Table 2.1(a)
Summary of the Area of Applicability of the MCNP5-1.51 Benchmark

Table Proprietary

Table 2.1(b)
Analysis of the MCNP5-1.51 calculations [3]

Table Proprietary

Table 2.1(c)



Table Proprietary

Table 5.1(a)



Table proprietary.



Table 5.1(b)



Table proprietary.



Table 5.1(c)

A large black rectangular redaction box covering the entire content of Table 5.1(c).

Table proprietary.

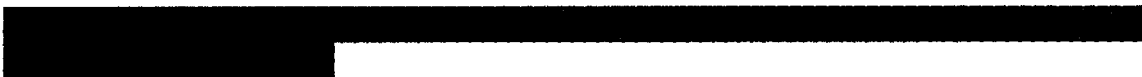
A large black rectangular redaction box covering the content of a table at the bottom of the page.

Table 5.1(d)



Table proprietary.

Table 5.1(e)



Table proprietary.



Table 5.2(a)
Reactor Core and Spent Fuel Pool Parameters

Table proprietary.



Table 5.2(b)
Reactor Control Blade Data

Table proprietary.

Table 5.2(c)



Table proprietary.



Table 5.3(a)
Fuel Rack Parameters and Dimensions

Table proprietary.

Table 5.3(b)
Fuel Rack Insert Parameters and Dimensions

Table proprietary.

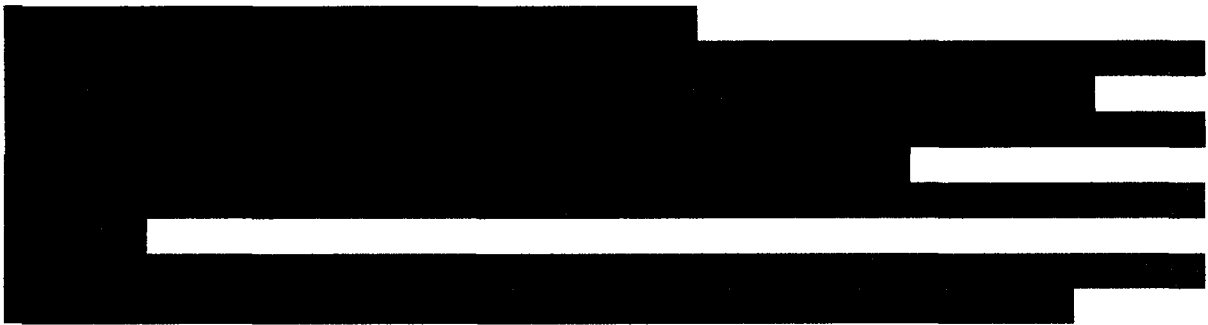


Table 5.4(a)
Non-Fuel Material Compositions

Table proprietary.



Table 5.4(b)
Summary of the Fuel and Fission Product Isotopes Used in Calculations

Table proprietary.

Table 7.1(a)



Table proprietary.

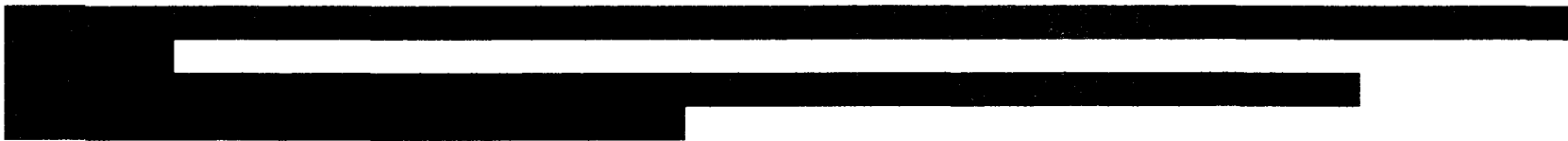


Table 7.1(b)



Table proprietary.



Table 7.1(c)



Table proprietary.



Table 7.2(a)
Results of the MCNP5-1.51 Calculations for SVEA-96 Optima2 QI22 Lattices

Description	Burnup (GWd/mtU)	k _{calc}	sigma	Max k _{calc}	delta k _{calc}	Uncertainty (95/95)
Lattice 146 (reference)	15	0.8599	0.0005	0.8740	Reference	Reference
	16	0.8660	0.0005			
	17	0.8702	0.0006			
	18	0.8740	0.0005			
	19	0.8733	0.0005			
	20	0.8733	0.0006			
	21	0.8678	0.0005			
Lattice 147 (void)	15	0.8502	0.0005	0.8660	-0.0081	0.0016
	16	0.8572	0.0005			
	17	0.8614	0.0005			
	18	0.8640	0.0006			
	19	0.8660	0.0006			
	20	0.8628	0.0005			
	21	0.8587	0.0005			
Lattice 147 (water) ^{††}	15	0.8493	0.0005	0.8643	-0.0097	0.0016
	16	0.8554	0.0005			
	17	0.8615	0.0005			
	18	0.8643	0.0005			
	19	0.8641	0.0006			
	20	0.8614	0.0005			
	21	0.8567	0.0005			
Lattice 148	15	0.8476	0.0005	0.8619	-0.0121	0.0016
	16	0.8538	0.0005			
	17	0.8591	0.0005			
	18	0.8601	0.0005			
	19	0.8619	0.0006			
	20	0.8600	0.0006			
	21	0.8553	0.0005			



Note 2: The maximum calculation uncertainty (sigma) used to determine the 95/95 delta k_{calc} may occur at an exposure which differs from that shown above.

Table 7.2(a) Continued

Description	Burnup (GWd/mtU)	k _{calc}	sigma	Max k _{calc}	delta k _{calc}	Uncert. (95/95)
Lattice 149 (void)	15	0.8389	0.0005	0.8533	-0.0207	0.0016
	16	0.8461	0.0005			
	17	0.8519	0.0005			
	18	0.8533	0.0005			
	19	0.8517	0.0005			
	20	0.8487	0.0006			
	21	0.8421	0.0005			
Lattice 149 (water) ††	15	0.8439	0.0005	0.8551	-0.0189	0.0016
	16	0.8516	0.0005			
	17	0.8551	0.0006			
	18	0.8548	0.0005			
	19	0.8524	0.0005			
	20	0.8476	0.0006			
	21	0.8400	0.0005			
Lattice 150	15	0.8464	0.0005	0.8587	-0.0154	0.0016
	16	0.8543	0.0005			
	17	0.8583	0.0005			
	18	0.8587	0.0005			
	19	0.8568	0.0006			
	20	0.8525	0.0005			
	21	0.8459	0.0005			
Lattice 151	15	0.8553	0.0005	0.8629	-0.0111	0.0016
	16	0.8611	0.0006			
	17	0.8629	0.0005			
	18	0.8622	0.0005			
	19	0.8591	0.0005			
	20	0.8537	0.0005			
	21	0.8477	0.0005			



Note 2: The maximum calculation uncertainty (sigma) used to determine the 95/95 delta k_{calc} may occur at an exposure which differs from that shown above.

Table 7.2(b)
Results of the MCNP5-1.51 Calculations for GE14 Lattice Type 5

Description	Burnup (GWd/mtU)	k_{calc}	sigma	delta k_{calc}	Uncert. (95/95)
SVEA-96 Optima2 QI22 lattice type 146	15.5	0.8991	0.0006	Reference	Reference
Single GE14	13	0.8447	0.0005	-0.0543	0.0016
Single GE14	13.5	0.8481	0.0005	-0.0509	0.0015
Single GE14	14	0.8500	0.0006	-0.0491	0.0016
Single GE14	14.5	0.8521	0.0005	-0.0469	0.0015
Single GE14	15	0.8517	0.0005	-0.0473	0.0015
Single GE14	15.5	0.8512	0.0005	-0.0479	0.0015
Single GE14	16	0.8505	0.0005	-0.0485	0.0015
Single GE14	16.5	0.8508	0.0005	-0.0482	0.0015
Single GE14	17	0.8491	0.0005	-0.0500	0.0015
2x2 GE14 - with channel (cell centered) (Case 2.3.1.5.4.1)	14.5	0.8517	0.0005	Reference	Reference
2x2 GE14 - no channel (Case 2.3.1.5.4.2)	14.5	0.8473	0.0006	-0.0044	0.0016
2x2 GE14 - no channel / eccentric center (Case 2.3.1.5.4.3)	14.5	0.8345	0.0005	-0.0173	0.0015
2x2 GE14 - no channel / eccentric out (Case 2.3.1.5.4.4)	14.5	0.8280	0.0005	-0.0238	0.0015

Note 2: The result of the SVEA-96 Optima2 QI22 lattice type 146 is provided as the reference.

Note 3: The maximum calculation uncertainty (sigma) used to determine the 95/95 delta k_{calc} may occur at an exposure which differs from that shown above.

Table 7.3
Results of the MCNP5-1.51 Calculations for Design Basis and Simplified Model of SVEA-96 Optima2 QI22 Lattice Type 146

Description	Burnup (GWd/mtU)	Code	k_{calc}	sigma
Simplified model of SVEA-96 Optima2 QI22 lattice 146 (Case 2.3.1.4.1)	15.5	CASMO-4	0.8890	N/A
Simplified model of SVEA-96 Optima2 QI22 lattice 146 (Case 2.3.1.4.2)	15.5	MCNP5-1.51	0.8985	0.0006
Model of SVEA-96 Optima2 QI22 lattice 146, similar to design basis [†] (Case 2.3.1.4.3)	15.5	MCNP5-1.51	0.8968	0.0005

Note 1: These calculations were performed using the design basis core operating parameters as indicated in Table 5.2(c).

Table 7.4
Results of the MCNP5-1.51 Calculations for Core Operating Parameters

Description	Power Density (W/gU)	Control Blade	Fuel Temp. (K)	Moderator Temp. (°F)	Void Fraction (%)	Burnup (GWd/mtU)	k_{calc}	sigma	delta k_{calc}	Uncert. (95/95)
Design basis (reference)	23.688	Yes	1176	547	0	15.5	0.8991	0.0006	Ref.	Ref.
Fuel temperature decreasing	23.688	Yes	588	547	0	16	0.8960	0.0006	-0.0030	0.0017
Moderator temperature decreasing	23.688	Yes	1176	528.8	0	15.5	0.8980	0.0005	-0.0011	0.0017
Void fraction increasing	23.688	Yes	1176	547	94	22	0.8859	0.0006	-0.0132	0.0017
Un-rodged operation	23.688	No	1176	547	0	17	0.8789	0.0005	-0.0202	0.0017
[REDACTED]	24.1617	Yes	1276	547	0	15.5	0.8987	0.0006	-0.0003	0.0017
[REDACTED]	24.1617	Yes	1376	547	0	15.5	0.8998	0.0006	0.0008	0.0017
[REDACTED]	20.1348	Yes	1176	547	0	15.5	0.8984	0.0005	-0.0007	0.0017

Note 1: The burnup calculations for core operating parameters were performed from 14 GWd/mtU to 24 GWd/mtU. For each core operating parameter, only reactivity of the burnup in this range which results in the largest reactivity is reported.

Note 2: The bounding case is bolded.

Note 3: The maximum calculation uncertainty (sigma) used to determine the 95/95 delta k_{calc} may occur at an exposure which differs from that shown above.

Table 7.5
Results of the MCNP5-1.51 Calculations for the Effect of Water Temperature and Density

Description	Burnup (GWd/mtU)	Water Temp. (°F)	Water Density (g/cc)	Temperature Adjustment, S(α,β) (°F)	k _{calc}	sigma	delta k _{calc}	Uncert. (95/95)
Reference: lower bound temperature (Case 2.3.2.1)	15.5	39.2	1	68.81	0.8991	0.0006	Reference	Ref.
Upper bound temperature for normal operation, low S(α,β) (Case 2.3.2.2)	15.5	150	0.98026	68.81	0.8950	0.0005	-0.0041	0.0015
Upper bound temperature for normal operation, high S(α,β) (Case 2.3.2.3)	15.5	150	0.98026	170.33	0.8924	0.0005	-0.0066	0.0015

Note 1: The maximum calculation uncertainty (sigma) used to determine the 95/95 delta k_{calc} may occur at an exposure which differs from that shown above.

Table 7.6(a)
Results of the MCNP5-1.51 Calculations for the Depletion Uncertainty

Description	k_{calc}	sigma	Depletion Uncertainty (5%)
Design basis	0.8991	0.0006	Reference
Fresh fuel, no Gd	1.0262	0.0006	0.0064

Table 7.6(b)



Table proprietary.

Table 7.7
Results of the MCNP5-1.51 Calculations for Fuel Tolerances

Description	Peak Reactivity Burnup (GWd/mtU)	k_{calc}	sigma	delta k_{calc} (95/95)	Max delta k_{calc} (95/95)
Design basis (reference)	15.5	0.8991	0.0006	Reference	Reference
Max fuel enrichment	16	0.9000	0.0005	0.0026	0.0026
Min fuel enrichment	15.5	0.8965	0.0005	-0.0009	
Max Gd loading	16	0.8961	0.0006	-0.0013	0.0038
Min Gd loading	15.5	0.9012	0.0005	0.0038	
Max pellet density	16	0.8974	0.0006	0.0000	0.0012
Min pellet density	15.5	0.8986	0.0006	0.0012	
Max pellet OD	15.5	0.8989	0.0006	0.0015	0.0015
Min pellet OD	16	0.8985	0.0005	0.0011	
Max clad ID	16	0.8984	0.0005	0.0010	0.0010
Min clad ID	16	0.8982	0.0005	0.0008	
Max clad OD	15.5	0.8971	0.0005	-0.0002	0.0027
Min clad OD	15.5	0.9001	0.0006	0.0027	
Max sub-bundle pitch	15	0.9072	0.0005	0.0098	0.0098
Min sub-bundle pitch	16.5	0.8884	0.0006	-0.0089	
Max pin pitch	15.5	0.9096	0.0006	0.0122	0.0122
Min pin pitch	15.5	0.8888	0.0006	-0.0086	
Max combined water wing canal inner width, channel outer square width, channel corner inner radius and central water canal inner square width	15	0.9005	0.0006	0.0031	0.0031
Min combined water wing canal inner width, channel outer square width, channel corner inner radius and central water canal inner square width	15.5	0.8963	0.0005	-0.0011	
Max combination of channel wall thickness and water cross wall thickness	16	0.8981	0.0006	0.0008	0.0019
Min combination of channel wall thickness and water cross wall thickness	15.5	0.8993	0.0006	0.0019	
Statistical combination of fuel tolerances					0.0171

Note 1: The maximum calculation uncertainty (sigma) used to determine the 95/95 delta k_{calc} may occur at an exposure which differs from that shown above.

Table 7.8
Results of the MCNP5-1.51 Calculations for Rack Tolerances

Description	Burnup (GWd/mtU)	k_{calc}	sigma	delta k_{calc} (95/95)	Max delta k_{calc} (95/95)
Design basis (reference)	15.5	0.8991	0.0006	Reference	Reference
Max cell ID Max cell pitch	15.5	0.8882	0.0006	-0.0093	N/A
Max wall thickness	15.5	0.9000	0.0005	0.0025	0.0025
Min wall thickness	15.5	0.8984	0.0005	0.0008	
Max insert width	15.5	0.8970	0.0005	-0.0005	0.0004
Min insert width	15.5	0.8979	0.0006	0.0004	
Statistical combination of rack tolerances					0.0026

Table 7.9(a)
Results of the MCNP5-1.51 Calculations for Fuel Radial Positioning in SFP Racks

Description	Burnup (GWd/mtU)	k_{calc}	sigma	delta k_{calc}	Unc. (95/95)
2x2 reference (Case 2.3.5.2.1)	15.5	0.8990	0.0005	Reference	Ref.
2x2 eccentric center (Case 2.3.5.2.2)	15.5	0.8937	0.0006	-0.0053	0.0015
2x2 eccentric in (Case 2.3.5.2.3)	15.5	0.8909	0.0005	-0.0081	0.0013
2x2 eccentric out (Case 2.3.5.2.4)	15.5	0.8943	0.0005	-0.0047	0.0014
2x2 insert/cell center (Case 2.3.5.2.5)	15.5	0.8992	0.0005	0.0002	0.0013
8x8 reference (Case 2.3.5.2.6)	15.5	0.8981	0.0005	Reference	Ref.
8x8 eccentric center (Case 2.3.5.2.7)	15.5	0.8958	0.0005	-0.0023	0.0014
8x8 eccentric in (Case 2.3.5.2.8)	15.5	0.8901	0.0006	-0.0080	0.0016
8x8 eccentric out (Case 2.3.5.2.9)	15.5	0.8946	0.0005	-0.0035	0.0014
8x8 insert/cell center (Case 2.3.5.2.10)	15.5	0.8997	0.0005	0.0016	0.0014
1x1 reference (Case 2.3.5.2.11)	15.5	0.8991	0.0006	Reference	Ref.
1x1 insert/cell center (Case 2.3.5.2.12)	15.5	0.8991	0.0006	0.0000	0.0015

Table 7.9(b)
Results of the MCNP5-1.51 Calculations for Fuel Orientation in SFP Racks

Description	Burnup (GWd/mtU)	k_{calc}	sigma	delta k_{calc}	Unc. (95/95)
Reference (Shown in Figure 2.9(a))	15.5	0.8990	0.0005	Reference	Ref.
Rotated fuel assembly (shown in Figure 2.9(b))	15.5	0.8982	0.0005	-0.0008	0.0014
Rotated fuel assembly (shown in Figure 2.9(c))	15.5	0.8983	0.0005	-0.0007	0.0014
Rotated fuel assembly (shown in Figure 2.9(d))	15.5	0.8977	0.0005	-0.0013	0.0013
Rotated fuel assembly (shown in Figure 2.9(e))	15.5	0.8983	0.0005	-0.0007	0.0013

Table 7.10

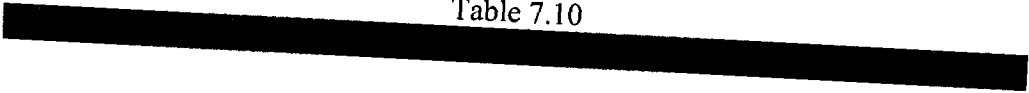


Table proprietary.

Table 7.11
Maximum k_{eff} Calculation for Normal Conditions in SFP Racks

Table proprietary.



Table 7.12(a)
Margin Evaluation

Results of the MCNP5-1.51 Calculations to Evaluate the Effect of Nominal Values Instead of Using Minimum B₄C Loading and Minimum Insert Thickness on Reactivity

Description	Burnup (GWd/mtU)	B-10 Areal Density (g/cm ²)	k _{calc}	sigma	delta k _{calc}
Reference (design basis) (Case 2.4.1)	15.5	0.0116	0.8991	0.0006	Reference
Rack with nominal values for B ₄ C loading and insert thickness (Case 2.4.2)	15.5	0.0133	0.8888	0.0005	-0.0103

Table 7.12(b)
Margin Evaluation
Results of the MCNP5-1.51 Calculations to Evaluate the Effect of the
Actual Optima2 QI22 Fuel Assembly

Description	Burnup (GWd/mtU)	k _{calc}	sigma	Max k _{calc}	delta k _{calc}
Optima2 QI22 Lattice 146 (Design basis) (Case 2.4.1)	15.5	0.8991	0.0006	Reference	Reference
Optima2 QI22 Lattice 147	15	0.8869	0.0005	0.8873	-
	15.5	0.8873	0.0005		
	16	0.8868	0.0005		
Optima2 QI22 Lattice 148	16	0.8834	0.0005	0.8843	-
	16.5	0.8843	0.0005		
	17	0.8825	0.0006		
Optima2 QI22 Lattice 149	14	0.8816	0.0005	0.8825	-
	14.5	0.8825	0.0005		
	15	0.8804	0.0006		
Optima2 QI22 Lattice 150	14	0.8859	0.0006	0.8863	-
	14.5	0.8863	0.0005		
	15	0.8856	0.0005		
Optima2 QI22 Lattice 151	14	0.8857	0.0005	0.8876	-
	14.5	0.8876	0.0006		
	15	0.8858	0.0005		
Optima2 QI22 Fuel Assembly [†] (Case 2.4.3)	Peak Reactivity Burnups (bolded)	0.8925	0.0006	0.8925	-0.0066

[†] The top and bottom natural blankets were conservatively neglected and replaced by adjacent lattice.

Table 7.12(c)
Margin Evaluation
Summary of the Margin Evaluation

Description	Value
Insert Composition Margin, from Table 7.12(a)	-0.0103
Actual Optima2 Fuel Assembly Margin, from Table 7.12(b)	-0.0066
Calculated Margin	-0.0169

Table 7.13(a)
Results of the MCNP5-1.51 Calculations for the Abnormal and Accident Conditions on
Reactivity of SFP

Table proprietary.

Note 1: The bounding accident is bolded.

Table 7.13(b)
Results of the MCNP5-1.51 Calculations for the Empty Storage Rack Cell without Insert

Description	Burnup (GWd/mtU)	k_{calc}	sigma	delta k_{calc}	Uncertainty (95/95)
Design basis (8x8 array)	15.5	0.8981	0.0005	Reference	Reference
Empty storage cell (cell centered)	15.5	0.8941	0.0006	-0.0041	0.0016
Empty storage cell (eccentric)	15.5	0.8900	0.0005	-0.0081	0.0014

Note 1: The design basis fuel assembly (Optima2 QI22 Lattice Type 146) is used for these calculations.

Table 7.14
Maximum k_{eff} Calculation for Abnormal and Accident Conditions in SFP Racks

Table proprietary.

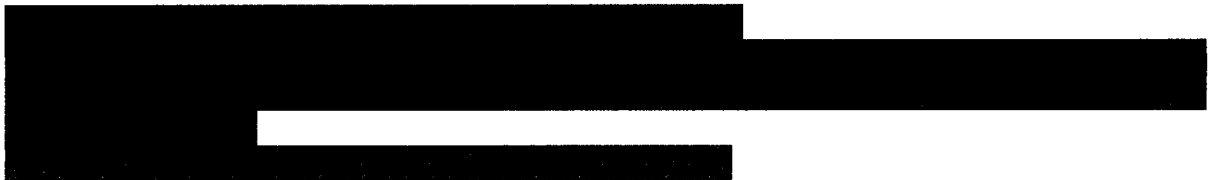


Table 7.15



Table proprietary.



Table 7.16
Results of the MCNP5-1.51 Calculations for Axially Infinite Optima2 QI22 Lattices

Description	Burnup (GWd/mtU)	k_{calc} (reference)	k_{inf} (infinite)	Delta-K	Uncertainty
Optima2 QI22 Lattice 146 (Design basis)	15.5	0.8991	0.9003	0.0013	0.0015
Optima2 QI22 Lattice 147	15.5	0.8873	0.8891	0.0018	0.0015
Optima2 QI22 Lattice 148	16.5	0.8843	0.8851	0.0008	0.0014
Optima2 QI22 Lattice 149	14.5	0.8825	0.8837	0.0011	0.0015
Optima2 QI22 Lattice 150	14.5	0.8863	0.8890	0.0027	0.0014
Optima2 QI22 Lattice 151	14.5	0.8876	0.8886	0.0010	0.0015

Note: The difference between the MCNP models under the “reference” column and the MCNP models under the “infinite” column is described in Section 5.1.

Table 7.17
Results of the MCNP5-1.51 Calculations for SFR Interface

Description	Burnup (GWd/mtU)	k_{calc}	sigma	delta k_{calc}	Uncertainty (95/95)
Design basis	15.5	0.8991	0.0006	Reference	Reference
Full SFP (cell centered)	15.5	0.8983	0.0006	-0.0008	0.0016
Full SFP (eccentric to SFP corner)	15.5	0.8938	0.0005	-0.0053	0.0015

Table 7.18



Table proprietary.

Figure proprietary.

Figure 2.1
2-D representation of the CASMO-4 models of SVEA-96 Optima2 QI22 lattices
(a) Lattice type 146; (b) lattice type 147; (c) lattice type 148;
(d) lattice type 149; (e) lattice type 150; (f) lattice type 151.

Figure proprietary.

Figure 2.2
2-D representation of the CASMO-4 models of GE14 lattices
(a) Lattice type 2; (b) lattice type 3; (c) lattice type 4;
(d) lattice type 5.

Figure proprietary

Figure 2.3
2-D representation of the CASMO-4 models of GE 8x8 lattices
(a) Lattice 854; (b) lattice 855.

Figure proprietary.

Figure 2.4
2-D representation of the CASMO-4 models of GE 7x7 lattices
(a) Lattice type V; (b) lattice type W.

Figure proprietary.

Figure 2.5
2-D representation of the CASMO-4 models of ATRIUM 9B lattices
(a) Lattice SPCA9-3.96L-10G6.5; (b) lattice SPCA9-3.96L-11G6.5;
(c) lattice SPCA9-3.96L-11G5.5.

Figure proprietary

Figure 2.6(a)
2-D representation of CASMO-4 SVEA-96 Optima2 QI22 model in the storage rack geometry.

Figure proprietary.

Figure 2.6(b)
2-D representation of MCNP5-1.51 SVEA-96 Optima2 QI22 model equivalent of the CASMO-4 model.

Figure proprietary.

Figure 2.6(c)
2-D representation of MCNP5-1.51 SVEA-96 Optima2 QI22 model used in criticality calculations.

Figure proprietary.

Figure 2.7
2-D representation of the MCNP5-1.51 SFP racks radial positioning for the 2x2 array models
(a) Cell centered positioning; (b) every fuel assembly is positioned toward the center; (c)
every fuel assembly is positioned toward the corner where the insert wings connect; (d)
every fuel assembly is positioned away from the corner where the insert wings connect;
(e) every fuel assembly is middle between insert and cell walls.

Figure proprietary.

Figure 2.8
2-D representation of the MCNP5-1.51 SFP racks radial positioning for the 8x8 array model
Every fuel assembly is positioned toward the center. Note that the insert is located in the
bottom left corner of every cell in the model.

Figure proprietary.

Figure 2.9
2-D representation of the MCNP5-1.51 fuel orientation in SFP rack cell for the 2x2 array models
(a) The reference case; (b) through (e) the other evaluated cases
One sub-lattice from each fuel assembly has a different color to show how fuel assemblies are rotated.

Figure proprietary

Figure 2.10(a)
A 2-D representation of the MCNP5-1.51 model of misloaded fuel assembly/missing insert
(eccentric).

Figure proprietary.

Figure 2.10(b)
A 2-D representation of the MCNP5-1.51 model of misloaded fuel assembly/missing insert (cell centered).

Figure proprietary.

Figure 2.11(a)
A 2-D representation of the MCNP5-1.51 model of mislocated fuel assembly in the corner
between two racks.

Figure proprietary.

Figure 2.11(b)
A 2-D representation of the MCNP5-1.51 model of mislocated fuel assembly in the corner
between two racks (eccentric).

Figure proprietary.

Figure 2.11(c)
A 2-D representation of the MCNP5-1.51 model of mislocated fuel assembly in the corner
between two racks (cell centered).

Figure proprietary.

Figure 2.12(a)
A 2-D representation of the MCNP5-1.51 model of mislocated fuel assembly adjacent to the platform (eccentric).

Figure proprietary.

Figure 2.12(b)
A 2-D representation of the MCNP5-1.51 model of mislocated fuel assembly adjacent to the platform (cell centered).

Figure proprietary.

Figure 2.13
2-D representation of the MCNP5-1.51 SFP racks radial positioning of the GE14 fuel assemblies
for the 2x2 array models
(a) Cell centered positioning with fuel channel; (b) Cell centered positioning without fuel
channel; (c) every fuel assembly without fuel channel is moved toward the center; (d) every fuel
assembly without fuel channel is moved away from the corner where the insert wings connect.

Figure proprietary.

Figure 5.1

A 2-D representation of the CASMO-4 model of the SVEA-96 Optima2 fuel lattice 146 in the core.

Figure proprietary.

Figure 5.2(a)
Quad Cities Unit 1 SFP.

Figure proprietary.

Figure 5.2(b)
Quad Cities Unit 2 SFP.

Figure proprietary.

Figure 5.3
Insert cross section profile.



Figure proprietary.

Figure 5.4
A 2-D representation of the MCNP5-1.51 model of the SFP rack cell with insert.

Figure proprietary.

Figure 7.1



Figure Proprietary

Figure 7.2



Figure Proprietary

Figure 7.3



Appendix A

Appendix proprietary.

Appendix B

Appendix proprietary.

Appendix C

Appendix proprietary

Supplement 1

Additional Calculations to Support the Revised NETCO-SNAP-IN[®] Rack Insert Design

(11 pages including this page)

S1.1 Introduction

This Supplement documents the criticality safety evaluation for the storage of spent BWR fuel in the Unit 1 and Unit 2 spent fuel pools (SFPs) at Quad Cities Station operated by Exelon. The purpose of this analysis is to justify that the specified changes in the NETCO-SNAP-IN[®] rack insert design [S1.1] are acceptable and bounded by the current analysis, presented in the main part of the report.

S1.2 Methodology

See Section 2 of the main report and as otherwise discussed below.

S1.3 Acceptance Criteria

See Section 3 of the main report.

S1.4 Assumptions

See Section 4 of the main report and as otherwise discussed below.

S1.5 Input Data

See Section 5 of the main report. The revised dimensions of the NETCO-SNAP-IN[®] rack insert are presented in Table S1-1 and Figure S1-1.

S1.6 Computer Codes

See Section 6 of the main report.

S1.7 Analysis

The comparison of the revised insert parameters presented in Table S1-1 with the previous insert design in Table 5.3(b) shows that changes are minor and therefore a significant impact on the conclusions made in the main part of the report is not expected. Nevertheless, to verify the negligible or minor impact of the revised insert design on results presented in the main part of the report additional calculations are presented in this Supplement. The additional calculations presented in this Supplement are similar to those in report for the following cases:

- SFP rack tolerances
- Fuel assembly radial positioning in the SFP rack
- Fuel orientation in the SFP rack

These cases are selected because the NETCO-SNAP-IN[®] rack insert design change may impact the reactivity in the rack. All other calculations from the main report are not affected by the NETCO-SNAP-IN[®] rack insert design change and the results of the unaffected calculations are

used in this Supplement where applicable. This approach is considered for both normal and accident conditions.

S1.7.1 SFP Rack Tolerances

As discussed in Section S1.7, the effect of the manufacturing tolerances on reactivity of the SFP racks with revised inserts was determined. The results of these calculations are presented in Table S1-2. The maximum positive delta-k value for each tolerance is statistically combined.

The maximum statistical combination of the SFP rack tolerances is used to determine k_{eff} in Table S1-5 and Table S1-6.

S1.7.2 Fuel Assembly Radial Positioning in the SFP Rack

As discussed in Section S1.7, twelve fuel assembly radial positioning cases in the racks were evaluated. The results of these calculations are presented in Table S1-3. For each eccentric position case, the result for similar but cell centered case is considered as a reference. The results show that most cases show a negative reactivity effect, however some delta k_{calc} values are positive. Therefore, a maximum delta k_{calc} value is applied as a bias and the correspondent 95/95 uncertainty is statistically combined with other uncertainties in Table S1-5 and Table S1-6.

S1.7.3 Fuel Orientation in the SFP Rack

As discussed in Section S1.7, five fuel assembly orientation cases in racks were evaluated. The results of these calculations are presented in Table S1-4. The result for the reference case is also included. The results show that all cases are statistically equivalent and the reactivity effect of fuel orientation is negligible. Nevertheless, a maximum positive delta k_{calc} value is applied as a bias and the correspondent 95/95 uncertainty is statistically combined with other uncertainties in Table S1-5 and Table S1-6.

S1.7.4 Maximum k_{eff} Calculations for Normal Conditions

The calculations of the maximum k_{eff} for normal conditions are described in Section 2.3.8 of the main part of the report. The results for the revised NETCO-SNAP-IN[®] rack insert design and the results from the main part of the report are tabulated in Table S1-5. The results show that the maximum k_{eff} for the normal conditions in the SFP racks is less than 0.95 at a 95% probability and at a 95% confidence level for the revised NETCO-SNAP-IN[®] rack insert design and are bounded by the results from the main part of the report.

S1.7.5 Maximum k_{eff} Calculations for Abnormal and Accident Conditions

The calculations of the maximum k_{eff} for accident conditions are described in Section 2.6 of the main part of the report. The bounding accident case from the main report is recalculated using the revised NETCO-SNAP-IN[®] rack insert design. The results for the revised NETCO-SNAP-IN[®] rack insert design and the results from the main part of the report are tabulated in Table S1-6. The results show that the maximum k_{eff} for abnormal and accident conditions in the SFP racks is less than 0.95 at a 95% probability and at a 95% confidence level for the revised NETCO-SNAP-IN[®] rack insert design and are bounded by the results from the main part of the report.

S1.8 References

[S1.1] Transmittal of Design Information NF1100434, Revision 1, "Quad Cities SFP Rack Insert Design Information", dated 09/11/2012.

S1.9 Conclusions

The criticality analysis for the storage of BWR assemblies in the Quad Cities SFP racks with revised NETCO-SNAP-IN[®] inserts has been performed. The results show that k_{eff} is [REDACTED] with the storage racks fully loaded with fuel of the highest anticipated reactivity, which is SVEA-96 Optima2 [REDACTED], at a temperature corresponding to the highest reactivity. The maximum calculated reactivity includes a margin for uncertainty in reactivity calculations with a 95% probability at a 95% confidence level. Reactivity effects of abnormal and accident conditions have been evaluated to assure that under all credible abnormal and accident conditions, the reactivity will not exceed the regulatory limit of 0.95.

The results show that the specified changes in the insert design are acceptable and bounded by the current analysis, presented in the main part of the report. [REDACTED]

[REDACTED] Therefore, any insert width dimension between the value used in the main report including the specified manufacturing tolerances and the value evaluated in this Supplement is acceptable.

Table S1-1
Fuel Rack Insert Revised Dimensions [S1.1]

Table proprietary.

[†] For the details of the insert dimensions, see Figure S1-1.

^{††} See Table 5.3(b)

Table S1-2
Results of the MCNP5 Calculations for Revised Rack Tolerances

Description	Burnup (GWd/mtU)	Filename	k_{calc}	sigma	delta k_{calc} (95/95)	Revised Max delta k_{calc} (95/95)	Reference Max delta k_{calc}[†] (95/95)
Design basis (reference)	15.5	op146-rt201155r	0.8963	0.0005	Reference	Reference	Reference
Max cell ID Max cell pitch	15.5	op146-rt202155r	0.8856	0.0005	-0.0091	0.0000	0.0000
Max wall thickness	15.5	op146-rt203155r	0.8964	0.0005	0.0017	0.0017	0.0025
Min wall thickness	15.5	op146-rt204155r	0.8958	0.0006	0.0011		
Max insert width	15.5	op146-rt206155r	0.8964	0.0005	0.0016	0.0030	0.0004
Min insert width	15.5	op146-rt207155r	0.8978	0.0005	0.0030		
Statistical combination of rack tolerances						0.0035	0.0026

† See Table 7.8

Table S1-3
Results of the MCNP5-1.51 Calculations for Revised Fuel Radial Positioning in SFP Racks

Description	Burnup (GWd/mtU)	Filename	k_{calc}	sigma	Revised delta k_{calc}	Revised Unc. (95/95)	Reference delta k_{calc} [†]	Reference Unc. [†] (95/95)
2x2 reference (Case 2.3.5.2.1)	15.5	2x2dbrot0155r	0.8954	0.0005	Ref.	Ref.	Ref.	Ref.
2x2 eccentric center (Case 2.3.5.2.2)	15.5	2x2ecnt155r	0.8926	0.0006	-0.0028	0.0015	-0.0053	0.0015
2x2 eccentric in (Case 2.3.5.2.3)	15.5	2x2ein155r	0.8900	0.0005	-0.0054	0.0015	-0.0081	0.0013
2x2 eccentric out (Case 2.3.5.2.4)	15.5	2x2eout155r	0.8940	0.0005	-0.0014	0.0015	-0.0047	0.0014
2x2 insert/cell center (Case 2.3.5.2.5)	15.5	2x2icnt155r	0.8956	0.0006	0.0001	0.0016	0.0002	0.0013
8x8 reference (Case 2.3.5.2.6)	15.5	8x8dbc155r	0.8966	0.0005	Ref.	Ref.	Ref.	Ref.
8x8 eccentric center (Case 2.3.5.2.7)	15.5	8x8ecnt155r	0.8934	0.0006	-0.0032	0.0015	-0.0023	0.0014
8x8 eccentric in (Case 2.3.5.2.8)	15.5	8x8ein155r	0.8895	0.0006	-0.0071	0.0015	-0.0080	0.0016
8x8 eccentric out (Case 2.3.5.2.9)	15.5	8x8eout155r	0.8931	0.0006	-0.0035	0.0016	-0.0035	0.0014
8x8 insert/cell center (Case 2.3.5.2.10)	15.5	8x8icnt155r	0.8975	0.0005	0.0009	0.0014	0.0016	0.0014
1x1 reference (Case 2.3.5.2.11)	15.5	op146- dbc155r	0.8963	0.0005	Ref.	Ref.	Ref.	Ref.
1x1 insert/cell center (Case 2.3.5.2.12)	15.5	1x1icnt155r	0.8967	0.0006	0.0004	0.0015	0.0000	0.0015

[†] See Table 7.9(a)

Table S1-4
Results of the MCNP5-1.51 Calculations for Revised Fuel Orientation in SFP Racks

Description	Burnup (GWd/mtU)	Filename	k_{calc}	sigma	Revised delta k_{calc}	Revised Unc. (95/95)	Reference delta k_{calc}[†]	Reference Unc.[†] (95/95)
Reference (Shown in Figure 2.9(a))	15.5	2x2dbrot0155r	0.8954	0.0005	Ref.	Ref.	Ref.	Ref.
Rotated fuel assembly (shown in Figure 2.9(b))	15.5	2x2dbrot1155r	0.8958	0.0005	0.0004	0.0014	-0.0008	0.0014
Rotated fuel assembly (shown in Figure 2.9(c))	15.5	2x2dbrot2155r	0.8965	0.0005	0.0011	0.0015	-0.0007	0.0014
Rotated fuel assembly (shown in Figure 2.9(d))	15.5	2x2dbrot3155r	0.8971	0.0005	0.0016	0.0014	-0.0013	0.0013
Rotated fuel assembly (shown in Figure 2.9(e))	15.5	2x2dbrot4155r	0.8978	0.0006	0.0024	0.0016	-0.0007	0.0013

[†] See Table 7.9(b)

Table S1-5
Maximum k_{eff} Calculation for Normal Conditions in Revised SFP Racks

Table proprietary.

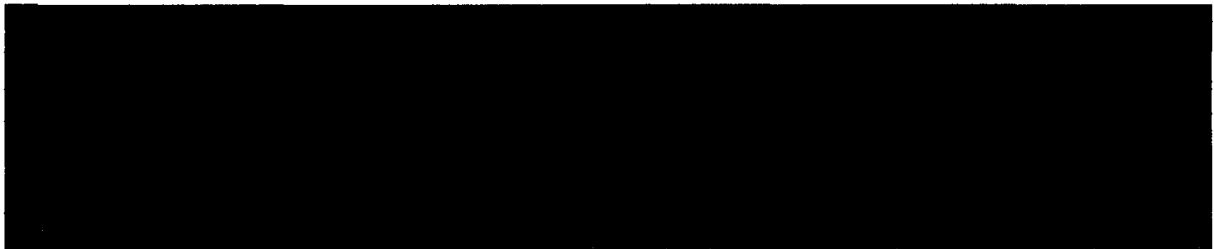


Table S1-6
Maximum k_{eff} Calculation for the Bounding Accident Condition in Revised SFP Racks

Table proprietary.

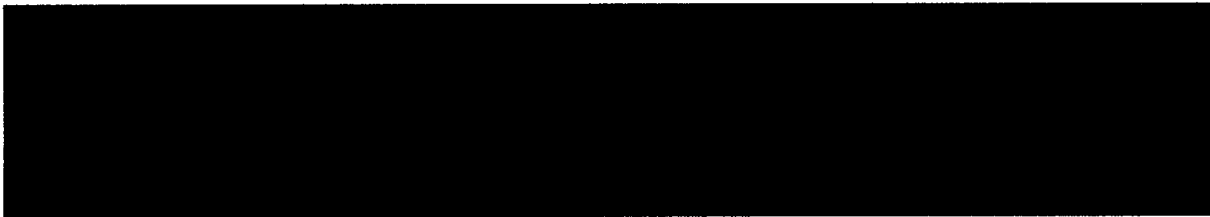


Figure proprietary.

Figure S1-1
Insert cross section profile [S1.1]

